

UNCLASSIFIED

Copy No. 1

~~RESTRICTED~~

RM No. L7G09



3 1176 00108 4079

~~RESTRICTED~~

To: UNCLASSIFIED

**NACA**By authority of *H. L. Dryden* Date *6-25-53**per naca Release form*  
*#1541. By HSR, 7-17-53.* 27 OCT 1947**RESEARCH MEMORANDUM**

INVESTIGATION OF HIGH-LIFT AND STALL-CONTROL DEVICES

ON AN NACA 64-SERIES 42° SWEEPBACK WING

WITH AND WITHOUT FUSELAGE

By

Robert R. Graham and D. William Conner

Langley Memorial Aeronautical Laboratory  
Langley Field, Va.

## CLASSIFIED DOCUMENT

This document contains classified information affecting the National Defense of the United States within the meaning of the Espionage Act, USC 5031 and 5032. Its transmission or the revelation of its contents in any manner to an unauthorized person is prohibited by law. Information so classified may be imparted only to persons in the military and naval services of the United States, appropriate civilian officers and employees of the Federal Government who have a legitimate interest therein, and to United States citizens of known loyalty and discretion who of necessity must be informed thereof.

**NATIONAL ADVISORY COMMITTEE  
FOR AERONAUTICS**

WASHINGTON

October 14, 1947

~~RESTRICTED~~**N A C A LIBRARY**LANGLEY MEMORIAL AERONAUTICAL  
LABORATORY  
Langley Field, Va.

UNCLASSIFIED

NACA RM L7G09

NATIONAL ADVISORY COMMITTEE FOR AERONAUTICS

RESEARCH MEMORANDUM

INVESTIGATION OF HIGH-LIFT AND STALL-CONTROL DEVICES

ON AN NACA 64-SERIES  $42^\circ$  SWEEPBACK WING

WITH AND WITHOUT FUSELAGE

By Robert R. Graham and D. William Conner

SUMMARY

An investigation has been conducted in the Langley 19-foot pressure tunnel on a  $42^\circ$  sweptback wing of aspect ratio 4, taper ratio 0.625, and with NACA 64-series airfoil sections to study several proposed devices for increasing the maximum lift coefficient and improving the longitudinal stability characteristics of sweptback wings at the stall. Devices investigated individually and in combination were leading-edge flaps and slats, trailing-edge split and extended split flaps, upper-surface split flaps, and upper-surface fences. The devices were investigated with and without a fuselage mounted on the wing. The Reynolds number for the test results presented was 6,840,000 but the effects of varying the Reynolds number through a range from 3,000,000 to 6,840,000 were also investigated on some configurations.

The results of the investigation indicate that a combination of leading-edge high-lift devices over the outer portion of the wing with trailing-edge flaps over the inner portion of the wing appears to offer a solution to the problem of obtaining a reasonable maximum lift coefficient and longitudinally stable characteristics at the stall for sweptback wings. Of the two leading-edge devices investigated, flap and slat, the leading-edge flap had the better characteristics. The maximum lift coefficient of the wing increased rapidly as the span of the outboard leading-edge flap was extended inboard, but a critical flap span exists beyond which further extensions inboard would result in unfavorable pitching-moment characteristics at the stall. For a given flap span the maximum lift coefficient increased above that for the wing alone as the wing was raised on the fuselage.

The installation of upper-surface fences for configurations with leading-edge devices improved the longitudinal stability characteristics just below the maximum lift coefficient but had little effect

beyond maximum lift. Outboard upper-surface flaps deflected up  $30^\circ$  improved the pitching-moment characteristics at the stall for those unstable configurations where only small positive pitching-moment increases occurred for angles of attack beyond the stall.

The leading-edge flaps caused the lateral-stability parameters to reach larger values near maximum lift by extending the linear range of the variation of the parameters with lift coefficient

Varying the Reynolds number from 3,000,000 to 6,800,000 had a negligible effect on the characteristics of the wing with leading-edge flap or slat.

### INTRODUCTION

Wind-tunnel tests in the Langley 19-foot pressure tunnel (reference 1) showed that a  $42^\circ$  sweptback wing of aspect ratio 4 and NACA 64<sub>1</sub>-112 airfoil sections was longitudinally unstable at the stall and also had relatively low values of maximum lift coefficient even with semispan split flaps. Preliminary tests of several devices which could be expected to increase the maximum lift coefficient or improve the stability characteristics at the stall showed promising results (reference 2); hence, the effects of these devices and additional devices have been studied in greater detail. The results of both investigations are summarized in the present report.

Devices investigated were leading-edge flaps and slats, trailing-edge split and extended split flaps, upper-surface split flaps, and upper-surface fences. The devices were investigated individually and in various combinations on the wing with and without a fuselage. The effects of the leading-edge flaps on the lateral stability characteristics of the wing with and without the fuselage were also investigated.

The main part of the investigation was conducted at a Reynolds number of 6,840,000 but the effects of varying the Reynolds number through a range from 3,000,000 to 6,840,000 were determined for some of the combinations.

### COEFFICIENTS AND SYMBOLS

All data are referred to the stability axes as shown in figure 1. The moments are referred to the quarter-chord point of the mean

aerodynamic chord of the wing regardless of fuselage location. The coefficients and symbols used in this report are defined as follows:

$C_L$	lift coefficient ( $L/qS$ )
$C_{L_{max}}$	maximum lift coefficient
$C_D$	drag coefficient ( $D/qS$ )
$C_Y$	lateral-force coefficient ( $Y/qS$ )
$C_l$	rolling-moment coefficient ( $L'/qSb$ )
$C_m$	pitching-moment coefficient ( $M/qSc$ )
$C_n$	yawing-moment coefficient ( $N/qSb$ )
$R$	Reynolds number ( $\rho Vc/\mu$ )
$M_o$	Mach number ( $V/a$ )
$\alpha$	angle of attack of root-chord line, degrees
$\psi$	angle of yaw, positive when right wing is back, degrees
$C_{l_\psi}$	rate of change of rolling-moment coefficient with angle of yaw ( $\partial C_l / \partial \psi$ ) per degree
$C_{n_\psi}$	rate of change of yawing-moment coefficient with angle of yaw ( $\partial C_n / \partial \psi$ ) per degree
$C_{Y_\psi}$	rate of change of lateral-force coefficient with angle of yaw ( $\partial C_Y / \partial \psi$ ) per degree
$L$	lift
$D$	drag
$Y$	lateral force
$L'$	rolling moment
$M$	pitching moment
$N$	yawing moment
$S$	wing area

- b wing span perpendicular to plane of symmetry
- $\bar{c}$  mean aerodynamic chord  $\frac{2}{S} \int_0^{b/2} c^2 dy$  measured parallel to plane of symmetry
- c local chord parallel to plane of symmetry
- y spanwise coordinate
- q free-stream dynamic pressure  $\left(\frac{1}{2}\rho V^2\right)$
- V free-stream velocity
- $\rho$  mass density of air
- $\mu$  coefficient of viscosity
- a velocity of sound
- $\delta_{fu}$  deflection of upper-surface flap

#### MODEL AND APPARATUS

The principal dimensions of the wing and fuselage are shown in figure 2. The wing has an angle of sweepback of  $42^\circ$  at the leading edge, an aspect ratio of 4.01, a taper ratio of 0.625, and airfoil sections of NACA 64 $\frac{1}{2}$ -112 perpendicular to the 0.273 chord line. The 0.273 chord line corresponds to the quarter-chord line of the panels before they were swept back. The tips are rounded off in both plan form and elevation beginning at  $0.975 \frac{b}{2}$ . The wing has no geometric dihedral or twist.

Details of the various high-lift and stall-control devices tested on the wing are shown in figure 3. The chord of the leading-edge flap (fig. 3(a)) was approximately 14.3 percent of the wing chord at the tip and 8.5 percent at the root. The  $\frac{1}{2}$ -inch-diameter tube at the leading edge of the flap was about the same radius as the average leading-edge radius of the wing. Figure 4 shows the flap installed on the wing. The slat (fig. 3(b)) had the same contour at the leading edge and on the upper surface as the basic wing. The wing was cut out to fit the lower surface of the slat so that in the retracted position the slat formed the leading edge of the wing. Figure 5 shows the slat installed on the wing.

The tapered leading-edge flap (fig. 3(c)) was designed to taper both in chord and in radius of curvature from zero chord and the wing-leading-edge radius at the inboard end ( $0.125 \frac{b}{2}$  station) to a chord of 0.21c and a radius of 0.30c at the outboard end ( $0.975 \frac{b}{2}$  station).

The normal split flaps (fig. 3(d)) extended over the inboard 50 percent of the wing span on the wing alone and on the low-wing fuselage combination. When the midwing and high-wing fuselages were in place, a section of the flap 12.3 percent of the wing span was removed at the center to allow clearance for the fuselage. The same flaps were also tested in an extended arrangement (fig. 3(e)) where the hinge line was moved to the wing trailing edge. The upper-surface flaps (fig. 3(f)) were similar to the normal split flaps except that they deflected from the upper surface over the outer portion of the wing.

The fences (fig. 3(g)) installed on the upper surface of the wing were mounted in a vertical plane parallel to the plane of symmetry.

A sharp leading edge on the inboard 50 percent of the wing span was simulated by a 1-inch-wide thin metal strip which formed an extension of the chord plane.

The fuselage (fig. 2) had circular cross sections and a fineness ratio of 10.2 to 1. The section of the fuselage intersected by the wing had a constant diameter. Percentages of this diameter were used to fix the three vertical locations of the wing root 0.273 chord point with respect to the fuselage center line. The locations were 37.5 percent below, 0 percent, and 37.5 percent above for the low-wing, midwing, and high-wing fuselage combinations, respectively. In each of the three positions the wing chord plane had a positive incidence of  $2^\circ$  with respect to the fuselage center line. No fillets were used in the wing-fuselage juncture. The high-wing fuselage combination is shown mounted for testing in figure 6.

#### TESTS

The tests were made in the Langley 19-foot pressure tunnel with the air in the tunnel compressed to  $2\frac{1}{3}$  atmospheres. To obtain the characteristics of the wing with the various high-lift and stall-control devices, measurements of lift, drag, and

pitching moment were made through a range of angle of attack of the wing from near zero lift to beyond maximum lift. Stall characteristics were studied by means of visual observations of tufts attached to the wing upper surface beginning at 20 percent of the wing chord. The tests were made at a Reynolds number of 6,840,000 and a Mach number of 0.14, but the effects of varying the Reynolds number through a range from 3,000,000 to 6,840,000 were determined for some configurations.

To obtain an indication of the effects of the leading-edge flaps on the lateral stability characteristics of the wing, measurements were made of the lift, rolling moment, yawing moment, and side force through a range of angles of attack at angles of yaw of  $0^\circ$  and  $\pm 5^\circ$ . Lift, drag, pitching-moment, rolling-moment, yawing-moment, and side-force measurements were also made through a range of angle of yaw, at an angle of attack of  $19.5^\circ$ . The yaw tests were made at a Reynolds number of 4,350,000 and a Mach number of 0.10.

The model mounted in the tunnel for the pitch tests is shown in figure 6(a) and for the yaw tests in figure 6(b).

## RESULTS AND DISCUSSION

The data presented herein have been corrected for tare and interference effects of the model supports and for jet-boundary effects as discussed in reference 1.

The results of the tests of the various high-lift and stall-control devices on the wing alone are summarized in table I and on the wing-fuselage combinations in table II. More complete data for some of the configurations tested are presented in figures 7 to 22.

### Characteristics of Wing with Various Devices

Leading-edge flaps.— The effects of the leading-edge flaps of various spans on the characteristics of the wing with and without trailing-edge flaps are shown in figure 7 and are summarized in table I. The leading-edge flaps extended the lift curve of the wing by delaying the stall to a higher angle of attack and, consequently, a higher lift coefficient. The increment in  $C_{l_{max}}$  increased rapidly as the span of the leading edge flap approached full wing span. When the leading-edge flaps covered only the outer

portion of the wing, the stall over that portion of the wing was delayed until after the inboard portion of the wing had stalled resulting in a stable pitching moment at the stall. (See fig. 8.) When the leading-edge flap extended over the full span of the wing, the stall was delayed over the entire span of the wing but the initial stall occurred at the wing tips resulting in an unstable stall similar to that of the wing without leading-edge flaps.

The positive slope of the pitching-moment-coefficient curve in the low-lift range was increased by the leading-edge flap by an amount that varied with flap span. The drag of the wing with or without trailing-edge flaps was increased in the low-lift range by the leading-edge flaps, but the increment of drag did not vary with leading-edge flap span. Near  $C_{L_{max}}$  the drag of the wing with  $0.575 \frac{b}{2}$ -span leading-edge flaps showed a rapid increase with lift coefficient, but as the span of the flaps was increased, the drag coefficient increased less rapidly with lift coefficient. (See fig. 7.)

The effects of cutting the ends of the flaps parallel to the air stream instead of perpendicular to the leading edge and of removing the clay fairing at the trailing edge of the flap (but still leaving the junction sealed) were found to be negligible. Varying the Reynolds number from 6,840,000 to 3,000,000 had a negligible effect on the characteristics of the wing with leading-edge flap.

Leading-edge slats with split flaps.— The effects of  $0.575 \frac{b}{2}$ -span slats combined with split flaps are shown in figures 9 and 10 and table I. At an angle of attack of  $16^\circ$ , a small area of stalled flow appeared at the inboard end of the slat accompanied by large areas of rough flow over the outer sections of the wing panels with resulting unfavorable changes in the aerodynamic characteristics. At this attitude, the lift-curve slope decreased abruptly, the drag coefficient increased rapidly, and the pitching-moment curve broke in an unstable direction. Beyond the first stall, a further increase in angle of attack brought about an increased area of inboard stall which caused the pitching-moment curve to reverse and have a stable slope through the maximum lift coefficient. The maximum lift coefficient was increased only a slight amount and the lift-curve peak was extremely flat. Measurements of the velocity gradient in the slat gap indicated that, near the wing surface, large losses in velocity occurred at angles of attack above  $14^\circ$ .

Installing the slats increased the drag of the wing throughout the lift range. Varying the Reynolds number from 6,840,000



to 3,000,000 had a negligible effect on the characteristics of the wing with slats extended.

Upper-surface fences.—Upper-surface fences tested on the unflapped wing produced no aerodynamic changes and therefore these data are not presented. When installed on the wing with slats extended, however, upper-surface fences improved the characteristics (fig. 9). Through a small range of angles of attack below stall, the cross flow was reduced, rough flow over the outer portions of the wing was delayed, and regions of separated flow were restricted to areas inboard of the fence. (See fig. 10.) As a result the unstable pitching-moment break below maximum lift was eliminated and the lift coefficient was increased about 0.1 at an angle of attack of  $25^\circ$ .

Upper-surface split flaps.—Outboard upper-surface flaps on the wing without leading-edge flaps improved the pitching-moment characteristics at the stall. Deflection of  $0.575 \frac{b}{2}$  span outboard upper-surface flaps caused a positive shift in pitching-moment coefficient in the low and moderate lift range (fig. 11). The effectiveness of the flap to produce a change in pitching moment decreased with increasing lift resulting in a stabilizing gradient of pitching moment. At the stall the effectiveness disappeared completely and with an up deflection of  $30^\circ$  the value of the pitching moment through the stall was constant. With this deflection the span of the flap was reduced to  $0.30 \frac{b}{2}$  span thereby decreasing the shift in pitching-moment coefficient in the low and moderate lift range without affecting the characteristics of the flap at the stall (fig. 12). Through most of the lift range below the stall the lift coefficient was reduced 0.12 and the drag coefficient was increased 0.024 by the addition of the  $0.30 \frac{b}{2}$  span upper-surface split flap deflected up  $30^\circ$ .

The data for these tests were obtained after the wing leading edge was modified to incorporate the retracted slat, and the maximum lift coefficient of the basic configuration was about 0.1 lower than that shown for the corresponding configuration in figure 7(b) (obtained before modification). The effects of the upper-surface flaps presented herein are believed to be unaffected by the wing modification.

During the tests extreme vibrations of the model were noted near maximum lift when the upper-surface flaps were deflected. The intensity of the vibrations increased as the span or deflection of the flap was increased.

Sharp leading edge.-- In tests of a  $60^\circ$  sweptback delta wing in the Langley full-scale tunnel, installing a sharp leading edge on the inboard sections of the wing brought about a large increase in the maximum lift coefficient. A similar installation on this wing of lower sweepback caused a reduction in  $C_{L_{max}}$  and had a destabilizing effect on the pitching-moment curve for the conditions of split flaps off or on. (See fig. 13.) The sharp leading edge reduced the maximum value of  $C_{L_{\psi}}$  and caused  $C_{n_{\psi}}$  to become positive near  $C_{L_{max}}$ .

### Wing-Fuselage Combinations

Characteristics with leading-edge flaps.-- Previous tests (reference 3) showed that the addition of the fuselage to the wing without leading-edge devices did not affect the characteristics of the wing near  $C_{L_{max}}$ . For the wing with leading-edge devices, however, where stalling occurred inboard, the presence of the fuselage had important effects on  $C_{L_{max}}$  and on the stability near  $C_{L_{max}}$ .

As in the case of the wing alone, the maximum lift coefficients of the wing-fuselage combinations increased rapidly when the span of the leading-edge flap was extended inboard and a span was reached beyond which further increases inboard resulted in unfavorable changes in the pitching-moment curve. (See table II and fig. 14.) This critical flap span which generally was lower than that for the wing alone ranged between  $0.575 \frac{b}{2}$  and  $0.725 \frac{b}{2}$ . The critical flap span was dependent on fuselage position and decreased as the wing was raised on the fuselage. The reason for the reduction in critical flap span by the presence of the fuselage may be seen in the stall diagrams for the wing with  $0.725 \frac{b}{2}$  flaps in figure 15.

The fuselage in midwing and high-wing positions produced similar effects on the stall progression by smoothing the flow over the inboard portion of the wing until stalling occurred at the tips, resulting in an unstable stall. With the fuselage in the low-wing position, stall initially occurred in the wing-fuselage juncture, resulting in a neutrally stable stall. The necessary decrease in flap span with changing fuselage position was counteracted by an increase in flap effectiveness with regard to increasing the maximum lift coefficient. Considering only flap spans which yielded satisfactory pitching-moment characteristics, the highest values of  $C_{L_{max}}$

possible for this wing with leading edge and split flaps and for the various fuselage combinations ranged from 1.44 to 1.55. (See table II.)

Adding the fuselage in the midwing or high-wing combinations decreased the drag coefficient as it did in the tests of reference 3 with split flaps on and leading-edge flaps off. Apparently a highly favorable interference effect exists for these wing-fuselage configurations when the split flaps are on the wing. Adding the fuselage in the low-wing position, however, increased the drag coefficient about 0.025. Unpublished data obtained from the tests of this model showed that with leading-edge flaps added to the low-wing fuselage combination, filling in the cut-out in the split flaps increased the drag coefficient about 0.015. If this effect were accounted for, the remaining increase in drag coefficient of 0.010 caused by the low-wing fuselage would be of the same magnitude as that observed in the tests of reference 3 and is probably due to adverse interference effects.

When upper-surface fences were added to the midwing fuselage combination with either the 0.575 or 0.725  $\frac{b}{2}$ -span leading-edge flaps (table II), the longitudinal-stability characteristics were improved just below the maximum lift coefficient as a result of restricting the stalled regions to areas inboard of the fences. With the 0.725  $\frac{b}{2}$ -span flaps, the maximum lift coefficient was increased but the fences were not effective enough to keep the final flow breakdown at 25° angle of attack from occurring at the wing tips, resulting in instability at the stall. An additional second pair of fences located at the 0.45  $\frac{b}{2}$ -span station did not improve the characteristics of this combination.

The results of tests with upper-surface flaps extending from the 0.4  $\frac{b}{2}$  to 0.7  $\frac{b}{2}$ -span stations and deflected up 30° on the midwing-fuselage combination with 0.725  $\frac{b}{2}$ -span leading-edge flaps are summarized in table II. The positive displacement in the pitching-moment coefficient caused by deflecting the upper-surface flaps, which decreased as the stall was approached, was not large enough to offset the final unstable break beyond the maximum lift coefficient. This arrangement of outboard split flaps therefore appears to improve the pitching-moment characteristics at the stall for unstable configurations where the change in pitching moment is only slightly positive.

An attempt was made to obtain higher  $C_{L_{max}}$  values while still controlling tip stall by testing a  $0.85 \frac{b}{2}$ -span leading-edge flap which tapered in chord from zero at the inboard end to about  $0.21c$  at the outboard end. The flap was tested on the wing with normal split flaps and the midwing fuselage. The results (table II) showed that the tapered flap did not increase  $C_{L_{max}}$  as much as the  $0.575 \frac{b}{2}$ -span leading-edge flap nor did it maintain stability at the stall. The addition of fences on the upper surface of the wing at the  $0.30$  and  $0.45 \frac{b}{2}$  stations, however, restricted the stalled areas and eliminated the instability at the stall.

Characteristics with slats.— The effects of the fuselage on the wing-slat combination were similar to those observed on the wing-leading-edge-flap combination where comparable data are available. (See table II and figs. 16 and 17.)

Tests of the slats with the split flaps removed were made with the midwing-fuselage combination only, and the results are presented in figures 18 and 19. The lift curve did not flatten in the high-lift range as it did with split flaps on, and the lift coefficient was still increasing at  $31^\circ$  angle of attack for the  $0.575 \frac{b}{2}$ -span slat. The effects of increasing the slat span to  $0.725 \frac{b}{2}$  were determined for the midwing-fuselage combination (figs. 19 and 20). The same effects were observed as for the corresponding leading-edge flap configurations with regard to an increase in the maximum lift coefficient and a decrease in the longitudinal stability at the stall.

Upper-surface fences had the same effects as were noted for the fuselage-off slat configuration and the fuselage-on, leading-edge-flap configurations.

The maximum lift coefficients for the slat-fence combinations were slightly greater than those for the leading-edge flaps of corresponding span, but they occurred at considerably higher angles of attack, as a result of a large decrease in lift-curve slope at a moderate angle of attack. Since the usable angles of attack for landing conditions are usually limited by geometrical considerations, a comparison of lift characteristics should be made at a constant angle of attack. On this basis the leading-edge flap was superior to the slat at angles of attack up to  $21^\circ$ . (See figs. 14, 17, and 19.)

Through most of the lift range the values of the drag coefficient for the slat-fence combinations were about 0.01 higher than those for the leading-edge flaps of corresponding span.

Yaw characteristics with leading-edge flaps.— The characteristics of the wing in yaw with  $0.725 \frac{b}{2}$ -span leading-edge flaps and semispan split flaps and the effects of a midwing fuselage on those characteristics are presented in figures 21 and 22. Comparison of figure 21 with corresponding data from reference 3 shows that the variation of the lateral-stability parameters,  $C_{l_\psi}$ ,  $C_{n_\psi}$ , and  $C_{Y_\psi}$  with lift coefficient is approximately the same for the wing with leading-edge flaps as for the wing without the leading-edge flaps but that the maximum values of these parameters were increased by an extension of the linear portion of the curves to a higher lift coefficient. The value of  $C_{l_\psi}$  obtained at a lift coefficient of 1.40 was 0.0056 corresponding to an effective dihedral of about  $50^\circ$  on wings of this plan form. The midwing fuselage had approximately the same effect on the lateral-stability parameters of the wing with leading-edge flap as on the parameters of the wing without leading-edge flaps.

#### CONCLUSIONS

The results of an investigation of several high-lift and stall-control devices on a  $42^\circ$  sweptback wing indicate the following conclusions:

1. A combination of leading-edge high-lift devices over the outer portion of the wing with trailing-edge flaps over the inner portion of the wing appears to offer a solution to the problem of obtaining a reasonable maximum lift coefficient and longitudinally stable characteristics at the stall for sweptback wings. Of the two leading-edge devices investigated, flap and slat, the leading-edge flap had the better characteristics.

2. The maximum lift coefficient of the wing increased rapidly as the span of the outboard leading-edge flap was extended inboard but a span was reached beyond which further increases inboard resulted in unfavorable changes in the pitching-moment curve. For a given flap span the maximum lift coefficient increased above that for the wing alone as the wing was raised on the fuselage.

3. The installation of upper-surface fences for configurations with leading-edge devices improved the longitudinal stability characteristics just below the maximum lift coefficient but had little effect beyond maximum lift.

4. Outboard upper-surface flaps deflected up  $30^\circ$  improved the pitching-moment characteristics at the stall for those unstable configurations where only small pitching-moment increases occurred for angles of attack beyond the stall.

5. The leading-edge flaps caused the lateral-stability parameters to reach larger values near maximum lift by extending the linear range of the variation of the parameters with lift coefficient.

6. Varying the Reynolds number from 3,000,000 to 6,800,000 had a negligible effect on the characteristics of the wing with leading-edge flap or slat.


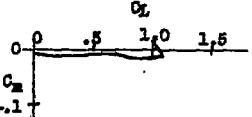

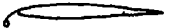




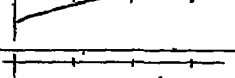

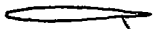
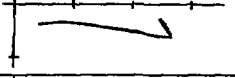


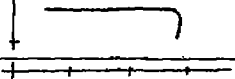

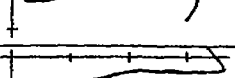

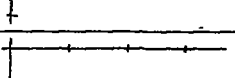
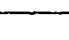

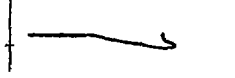

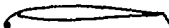
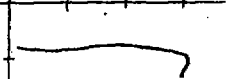

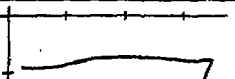

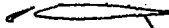
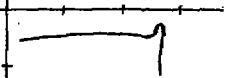

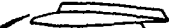
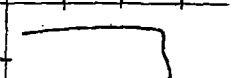

Langley Memorial Aeronautical Laboratory  
National Advisory Committee for Aeronautics  
Langley Field, Va.

#### REFERENCES

1. Neely, Robert H., and Conner, D. William: Aerodynamic Characteristics of a  $42^\circ$  Swept-Back Wing with Aspect Ratio 4 and NACA 64<sub>1</sub>-112 Sections at Reynolds Numbers from 1,700,000 to 9,500,000. NACA RM No. L7D14, 1947.
2. Conner, D. William, and Neely, Robert H.: Effects of a Fuselage and Various High-Lift and Stall-Control Flaps on Aerodynamic Characteristics in Pitch of an NACA 64-Series  $40^\circ$  Swept-Back Wing. NACA RM No. L6L27, 1947.
3. Salmi, Reino J., Conner, D. William, and Graham, Robert R.: Effects of a Fuselage on the Aerodynamic Characteristics of a  $42^\circ$  Sweptback Wing at Reynolds Numbers to 8,000,000. NACA RM No. L7E13, 1947.

TABLE I.- EFFECTS OF SEVERAL HIGH-LIFT AND STALL-CONTROL DEVICES ON THE CHARACTERISTICS  
OF A 42° SWEEPBACK WING WITH NACA 64<sub>1</sub>-112 AIRFOIL SECTIONS; FUSELAGE OFF

[R = 6,840,000]

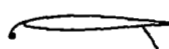
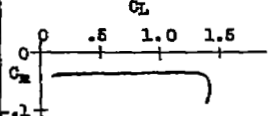

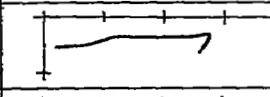

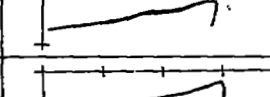
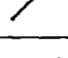
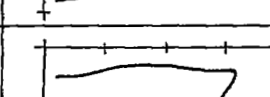

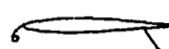
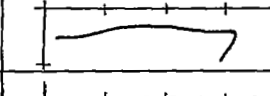
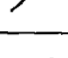
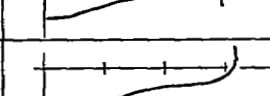
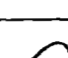
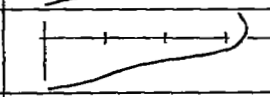

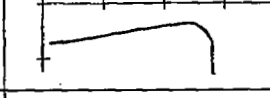

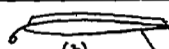
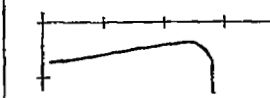

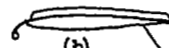
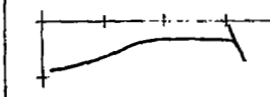

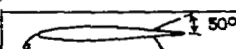
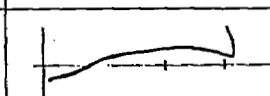

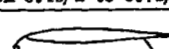
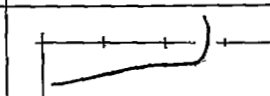

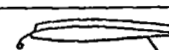
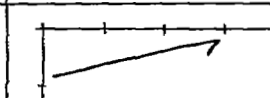

Configuration	Span of L.E. flap or slat (b/2) (a)	$C_{L_{max}}$	$\alpha_{C_{L_{max}}}$ (deg)	D/L at $0.85C_{L_{max}}$	$C_m$ characteristics	Type of $C_L$ peak	Fig. no.
	Off	1.10	19	0.095			7(a)
	0.575	1.24	25	.137			7(a)
	.725	1.50	27	.125			7(a)
	.975	1.80	27	.134			7(a)
	Off	1.30	16.4	.188			7(b)
	.575	1.40	19	.161			7(b)
	.725	1.58	24	.160			7(b)
	.975	1.79	25	.165			7(b)
	Off	1.40	16	.145			Reference 2
	.575	1.52	19	.155			Reference 2
	.725	1.75	24	.170			Reference 2
	.575	1.55	19	.154			9
 Fences at 0.45 b/2	.575	1.41	25	.157			9

\* Outboard end of L.E. flap or slat at 0.975 b/2.

NATIONAL ADVISORY  
COMMITTEE FOR AERONAUTICS

TABLE II.—EFFECTS OF A FUSELAGE ON THE CHARACTERISTICS OF A  $42^\circ$  SWEEPBACK WING WITH  
NACA 64<sub>1</sub>-112 AIRFOIL SECTIONS AND SEVERAL HIGH-LIFT AND STALL-CONTROL DEVICES

[ $R = 6,840,000$ ]

Configuration (a)	Fuselage location	$C_{L_{max}}$	$\alpha_{C_{L_{max}}}$	D/L at $0.85C_{L_{max}}$	$C_m$ characteristics	Type of $C_L$ peak	Fig. no.
 0.575b/2-span L.E. flap	Off	1.40	19	0.151			14(a)
	Low-wing	1.59	19	.161			14(a)
	Midwing	1.44	21	.164			14(a)
	High-wing	1.52	25	.178			14(a)
 0.725b/2-span L.E. flap	Off	1.56	24	.160			14(b)
	Low-wing	1.55	21	.168			14(b)
	Midwing	1.56	24	.160			14(b)
	High-wing	1.66	25	.168			14(b)
 (b) 0.575b/2-span L.E. flap	Midwing	1.42 <sup>a</sup>	21	.163			—
 (b) 0.725b/2-span L.E. flap	Midwing	1.66	25	.175			—
 0.725b/2-span L.E. flap Upper surface flap from 0.4b/2 to 0.7b/2	Midwing	1.57	25	.188			—
 Tapered L. E. flap	Midwing	1.37	19.5	.145			—
 Tapered L. E. flap Fences at 0.50b/2 and 0.45b/2	Midwing	1.45	19.5	.156			—

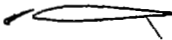
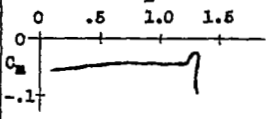
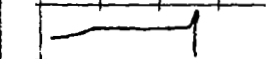
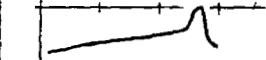
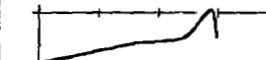
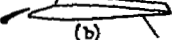
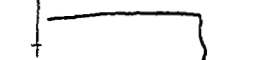
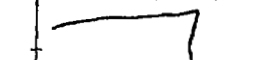
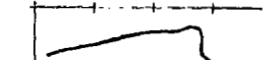
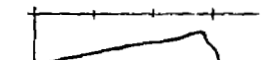
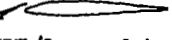
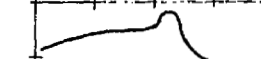
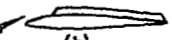
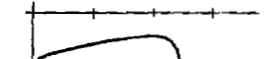
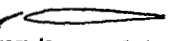


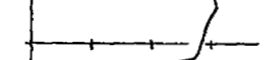
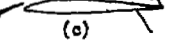
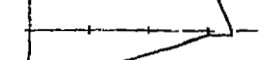
<sup>a</sup> Outboard end of L.E. flap at 0.975b/2

<sup>b</sup> Fences located 0.05b/2 outboard of inboard end of L.E. flap

NATIONAL ADVISORY  
COMMITTEE FOR AERONAUTICS



TABLE II.—EFFECTS OF A FUSELAGE ON THE CHARACTERISTICS OF A  $12^\circ$  SWEEPBACK WING — Concluded[ $R = 6,840,000$ ]

Configuration (a)	Fuselage location	$C_{L_{max}}$	$C_{D_{max}}$	D/L at $0.85C_{L_{max}}$	$C_m$ characteristics	Type of $C_L$ peak	Fig. no.
 0.575b/2-span slat	Off	1.35	19	0.154			16
	Low-wing	1.32	22	.162			16
	Midwing	1.48	51	.169			16
	High-wing	1.48	28	.175			16
 (b) 0.575b/2-span slat	Off	1.41	25	.157			17
	Low-wing	1.45	51	.172			17
	Midwing	1.52	51	.195			17
	High-wing	1.55	28	.193			17
 0.575b/2-span slat	Midwing	1.45	51	.280			18
 (b) 0.575b/2-span slat	Midwing	1.48	51	.266			18
 0.725b/2-span slat	Midwing	1.48	29	.200			19
 0.725b/2-span slat	Midwing	1.54	28	.172			19
 (c) 0.725b/2-span slat	Midwing	1.68	28	.202			19

<sup>a</sup> Outboard end of slat at  $0.975b/2$ <sup>b</sup> Fences located  $0.05b/2$  outboard of inboard end of slat<sup>c</sup> Fences located  $0.05b/2$  and  $0.20b/2$  outboard of inboard end of slatNATIONAL ADVISORY  
COMMITTEE FOR AERONAUTICS

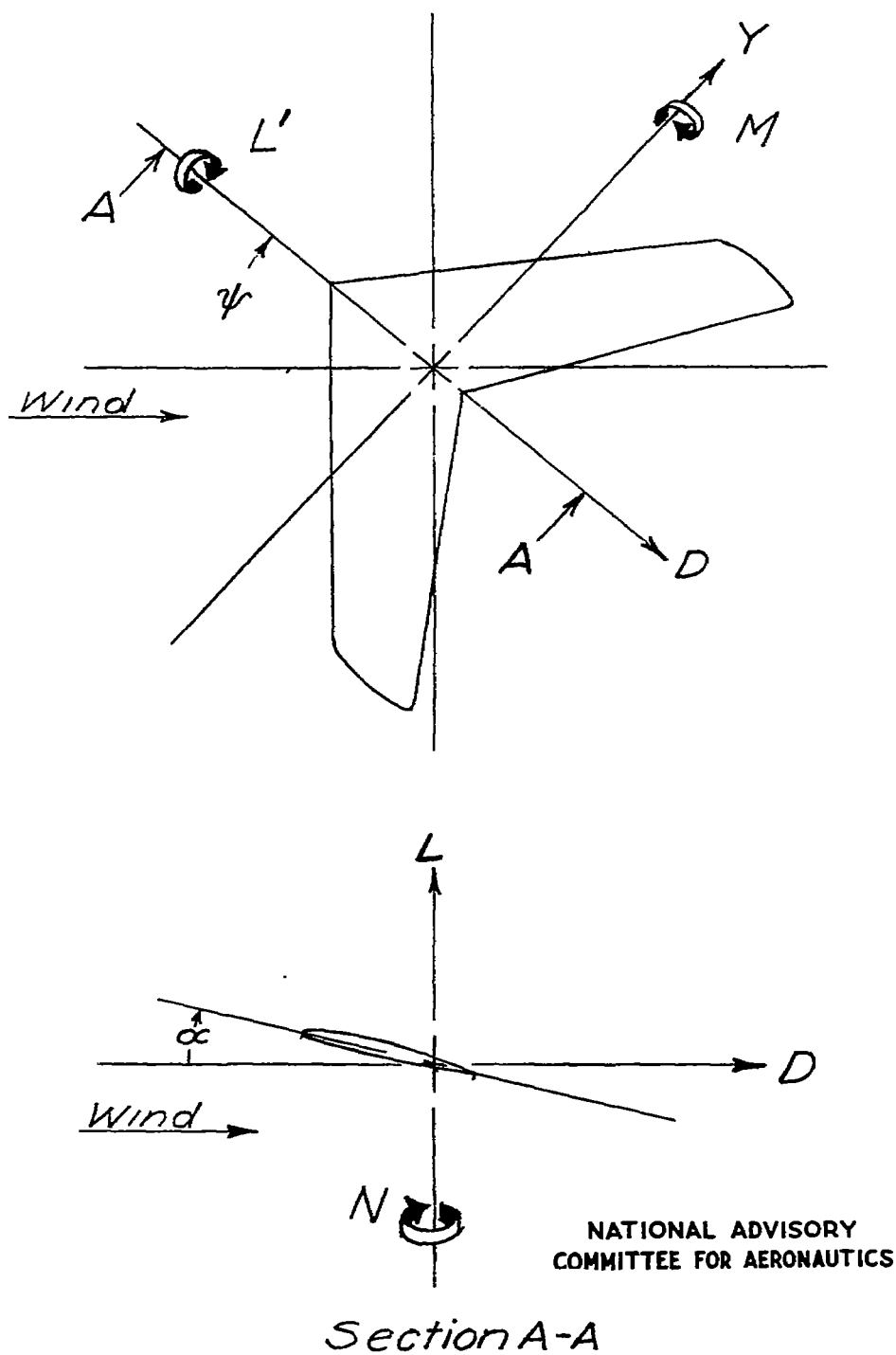
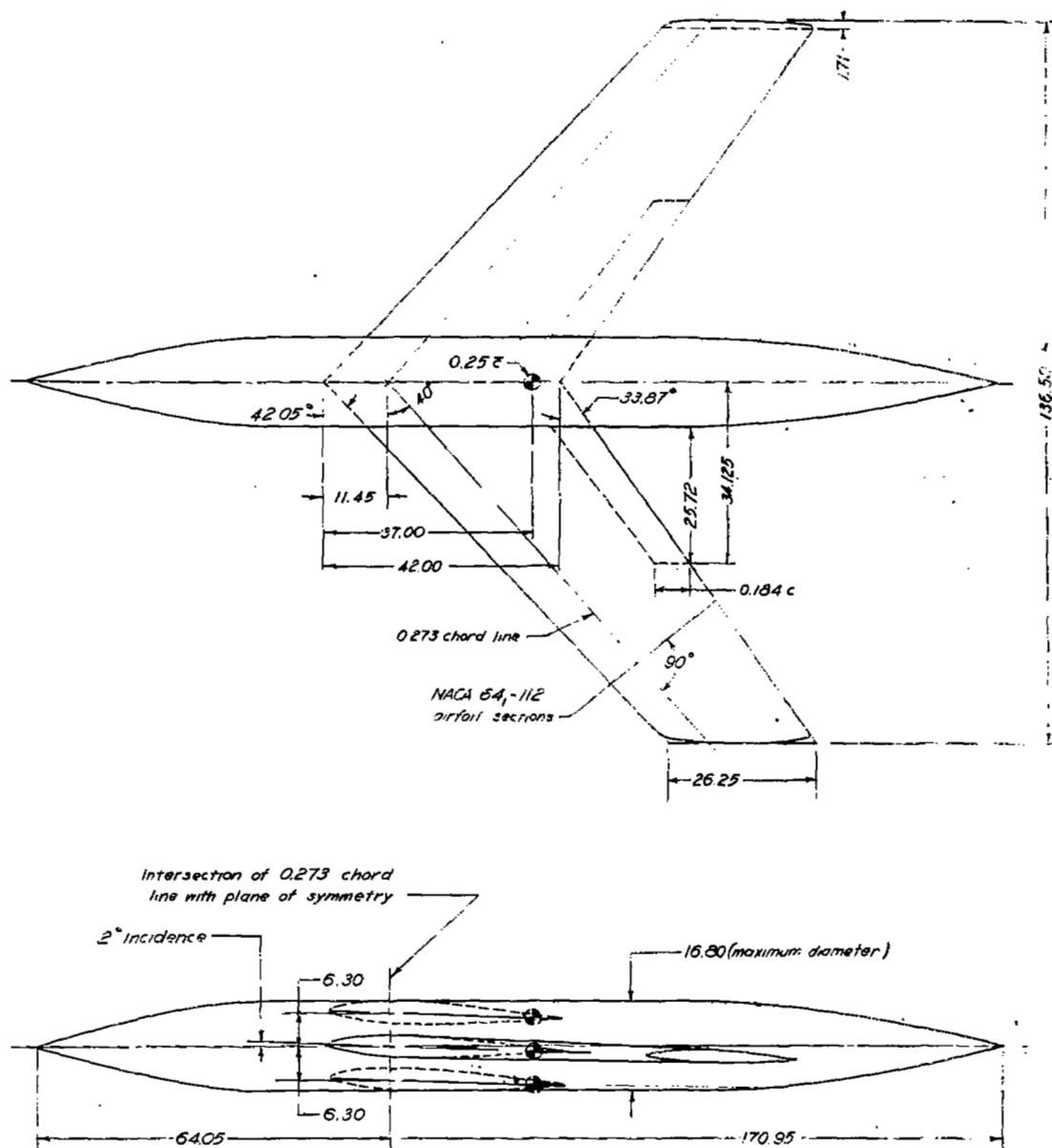


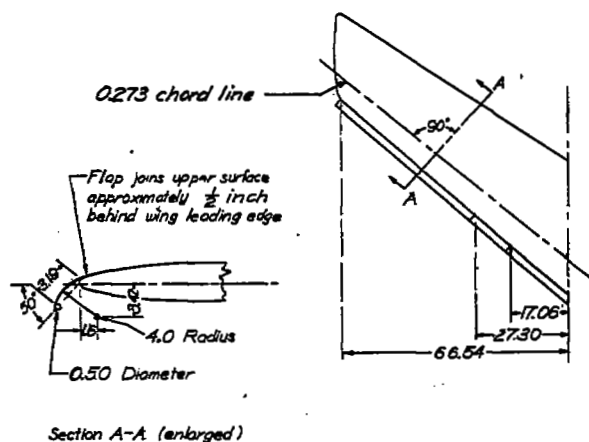
Figure 1.- System of axes.



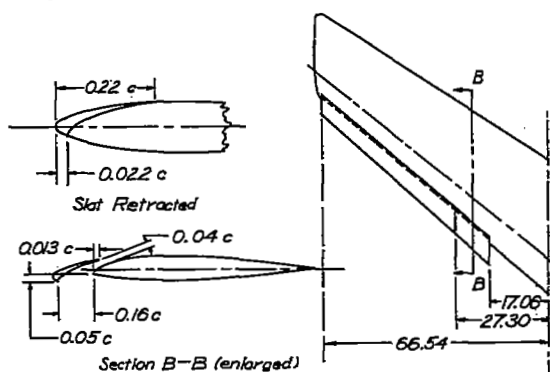
FUSELAGE ORDINATES			
Distance behind fuselage nose	Fuselage diameter	Distance behind fuselage nose	Fuselage diameter
0	0.20	112.00	16.80
16.00	9.84	122.00	16.32
22.05	11.80	132.00	14.90
27.39	13.80	142.00	12.52
34.56	15.60	151.20	9.46
42.35	16.60	162.00	4.78
48.00	16.80	170.95	0

NATIONAL ADVISORY  
COMMITTEE FOR AERONAUTICS

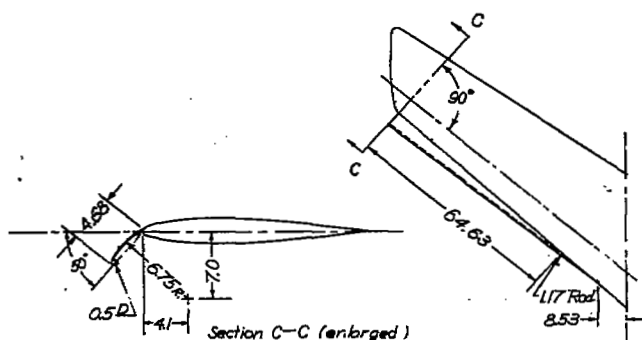
Figure 2.- Geometry of 42° swept-back wing and fuselage. Aspect ratio = 4.01; taper ratio = 0.625; area = 4643 sq in.;  $\bar{c}$  = 34.7 in. No dihedral or twist. (All dimensions in inches.)



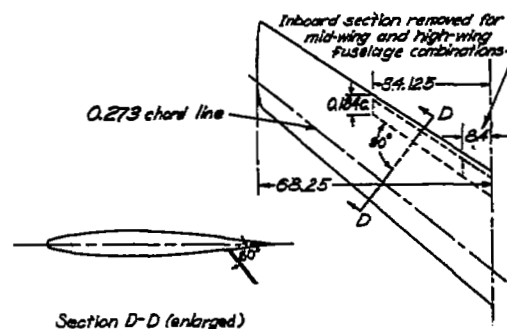
(a) Leading-edge flap



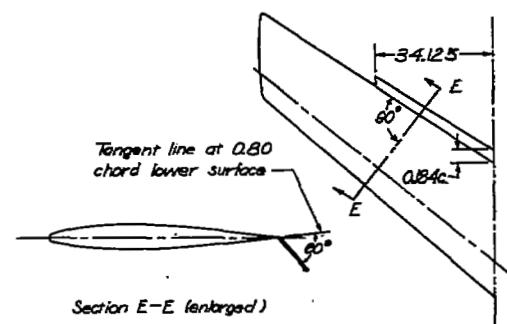
(b) Slat



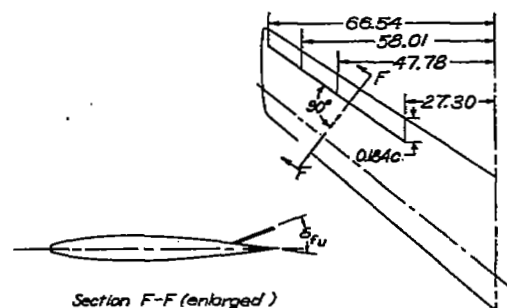
(c) Tapered leading-edge flap



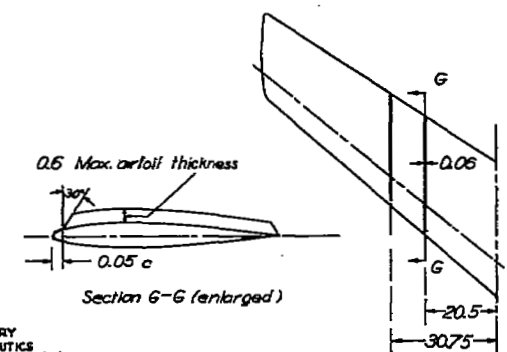
(d) Normal split flap



(e) Extended split flap



(f) Upper surface flap



(g) Upper surface fences

Figure 3.-Details of high-lift and stall-control devices on 42° sweptback wing

100  
100  
100  
100

100

100

100

100

100

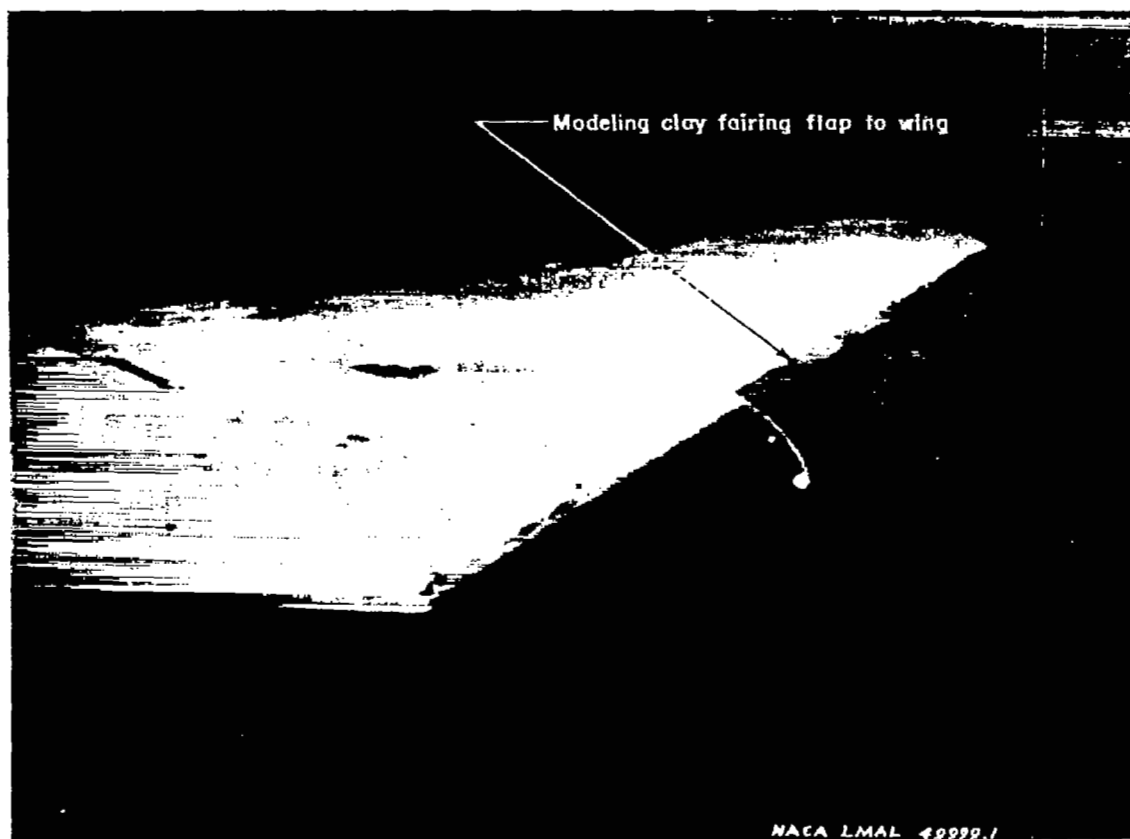


Figure 4.- Leading-edge flap mounted on wing.

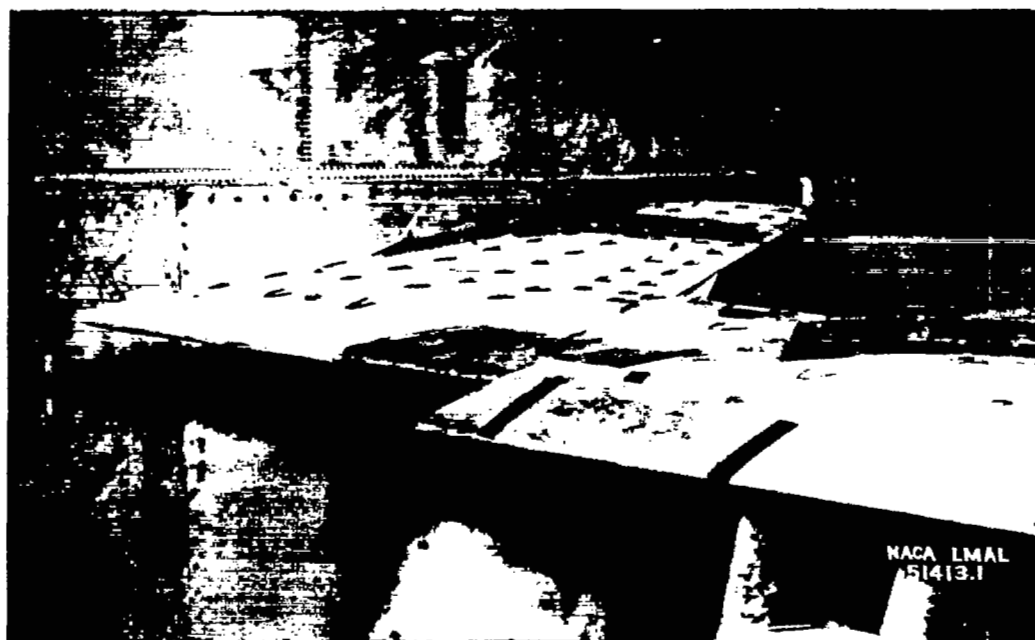
100

100

100



(a)  $0.725 \frac{b}{2}$ -span slat on wing with midwing fuselage.



(b)  $0.575 \frac{b}{2}$ -span slat and upper surface fences on wing alone.

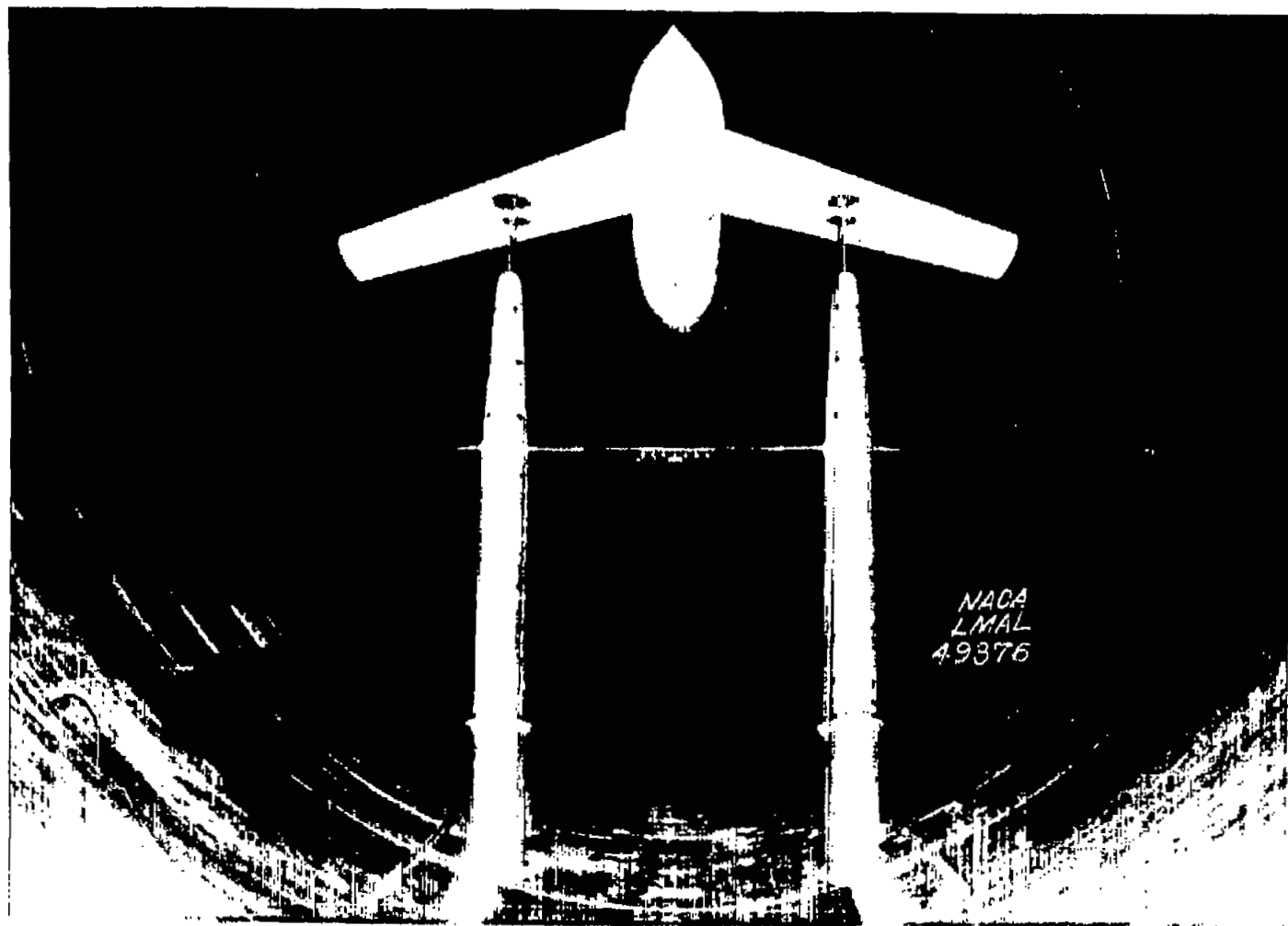
Figure 5.- Installation of slat on wing.



1  
2  
3  
4

5  
6  
7

8  
9  
10  
11



(a) Front view of high-wing fuselage combination on normal supports.

Figure 6.- Model mounted in Langley 19-foot pressure tunnel.

100

100

100

100

100

100

100

100

100

100

100

100

100

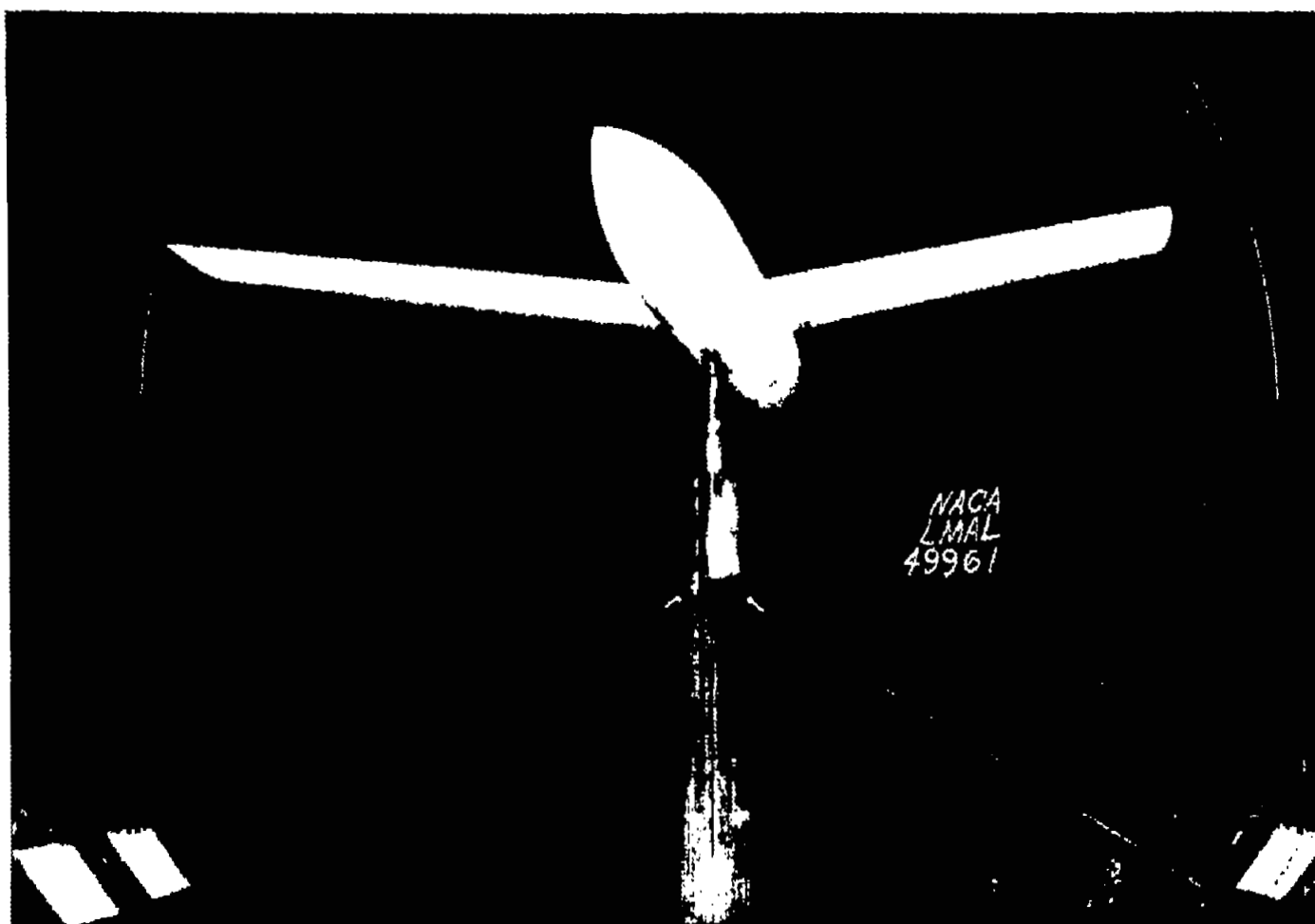
100

100

100

100

100



(b) Rear view of midwing fuselage combination on yaw support.

Figure 8.- Concluded.

10  
11  
12  
13

14

15  
16

17

18

19

20

21

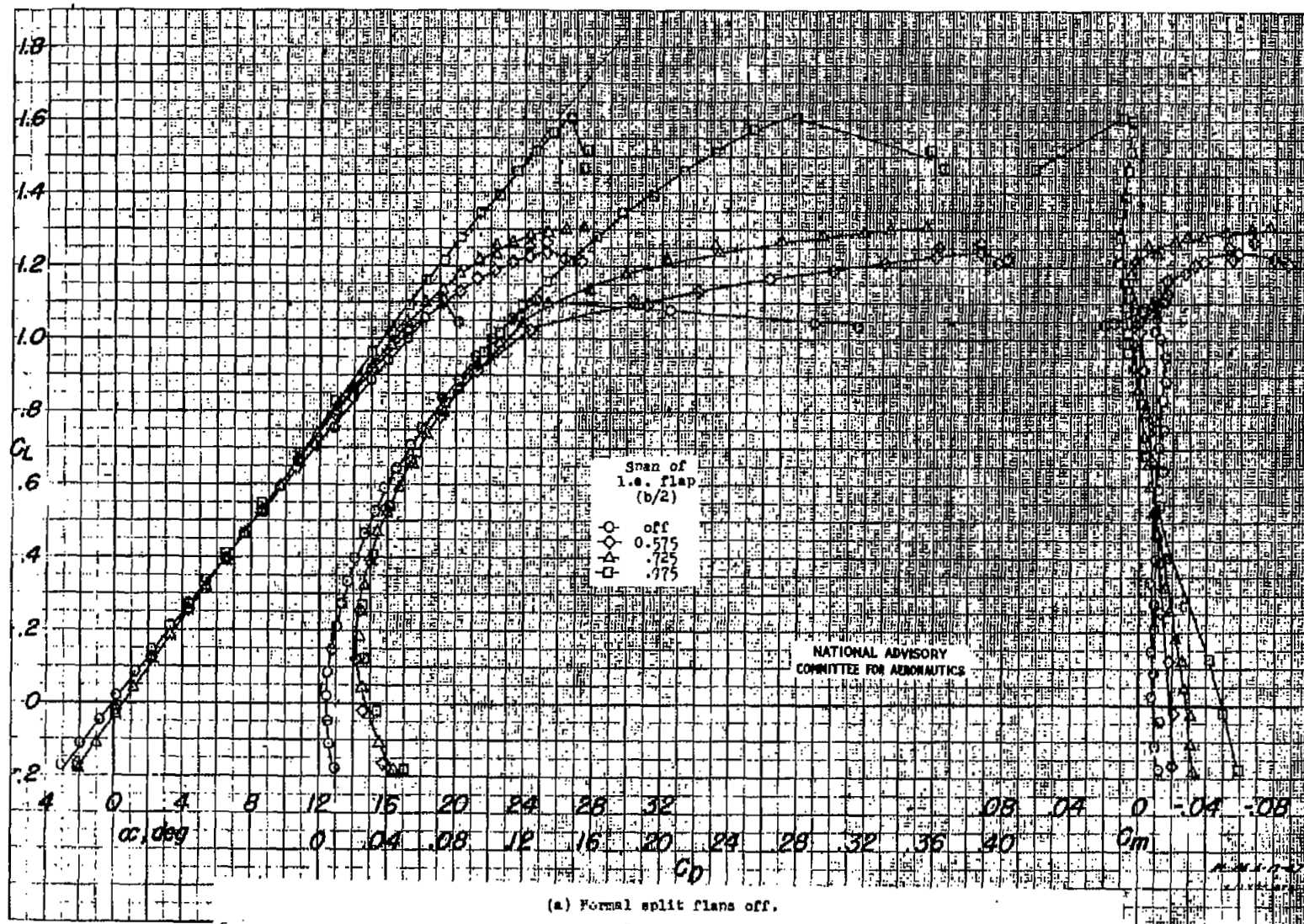
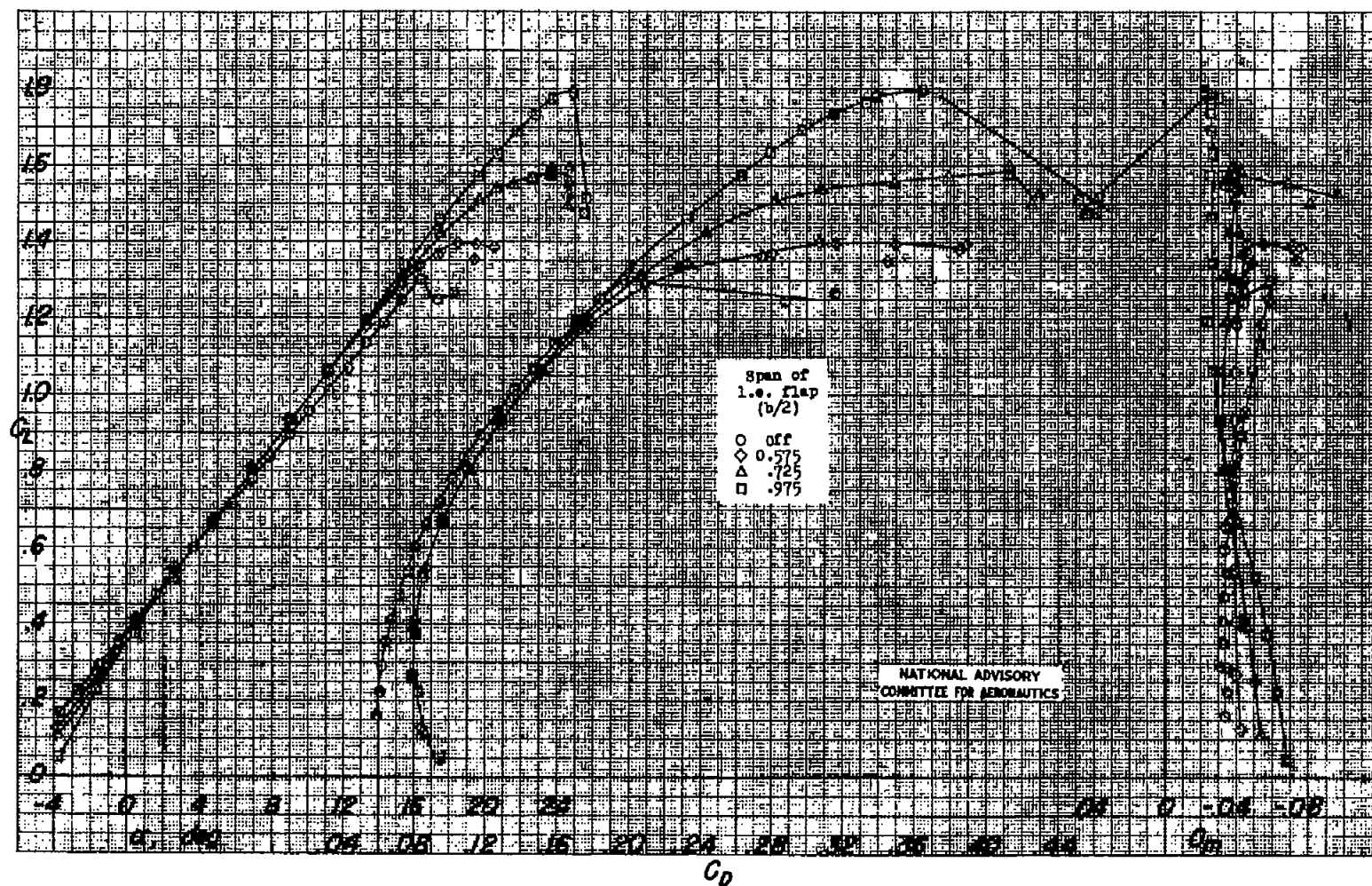


Figure 7.- Aerodynamic characteristics of a  $42^\circ$  sweptback wing with a leading edge flap of various spans.  $R = 6,240,000$ .



(b) Normal split flaps on.

Figure 7.- Concluded.

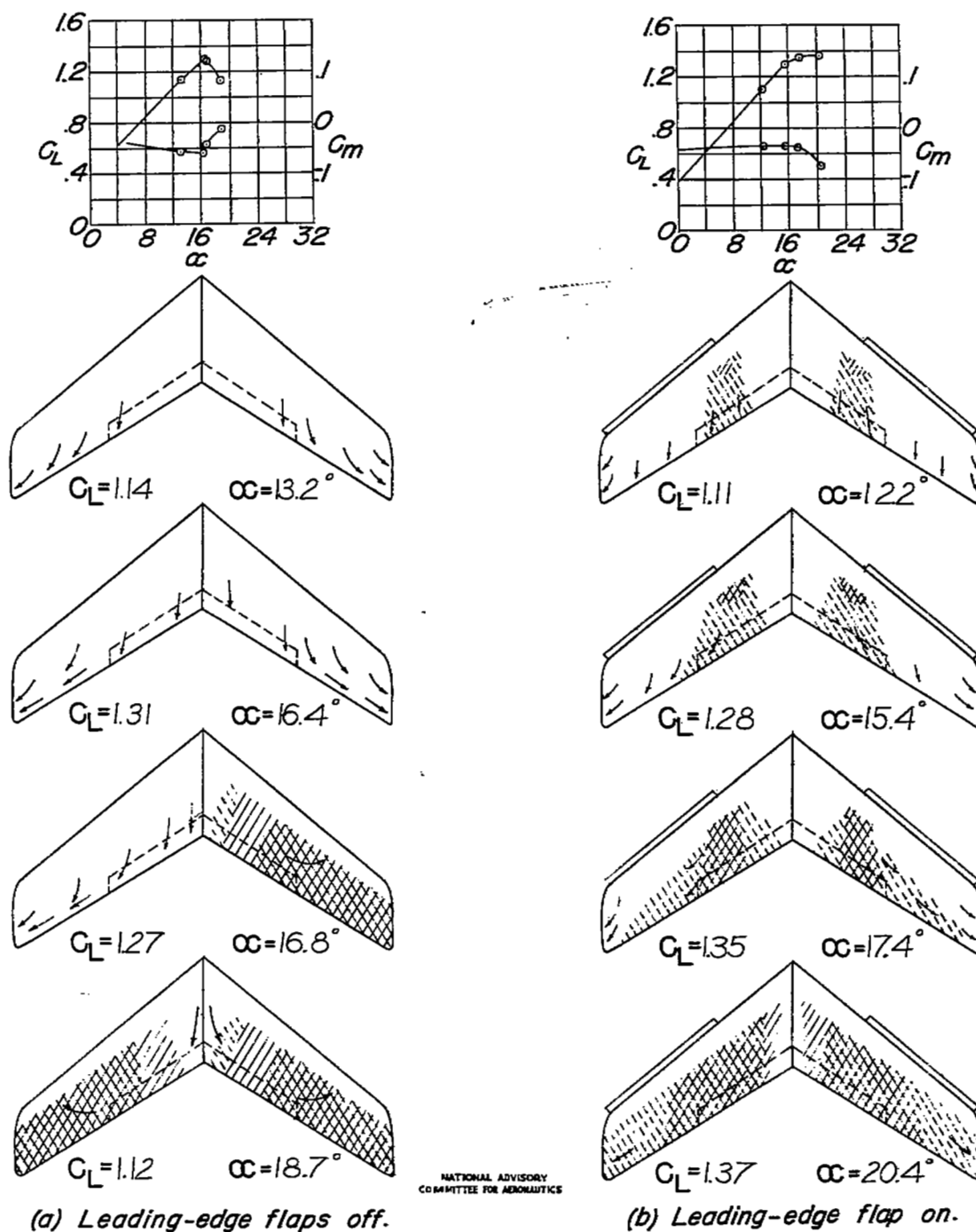
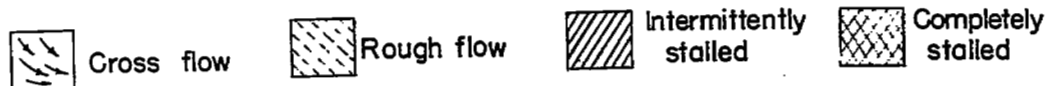
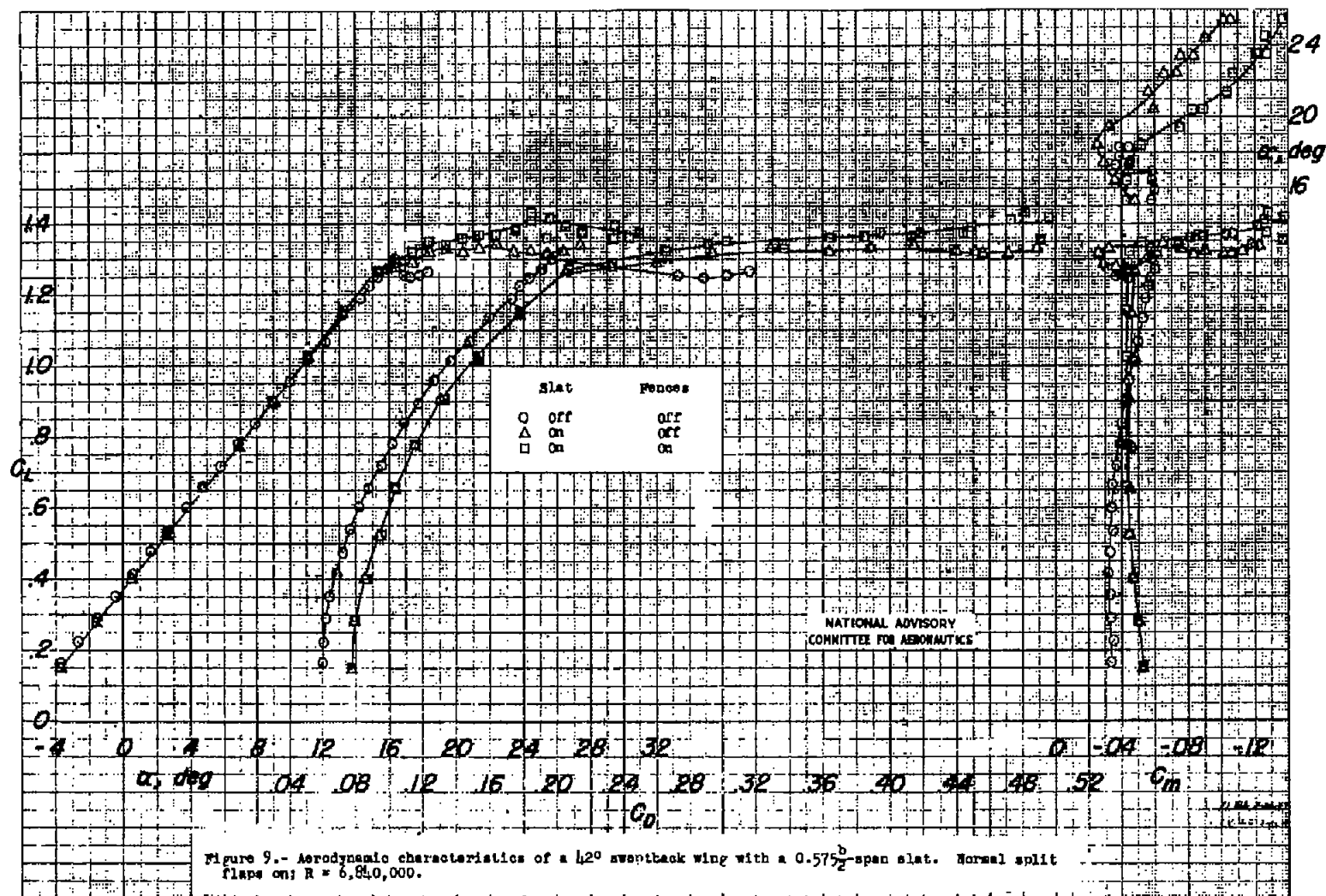
NATIONAL ADVISORY  
COMMITTEE FOR AERONAUTICS

Figure 8.— Effect of  $0.575 \frac{b}{2}$  span leading-edge flap on stalling characteristics of  $42^\circ$  sweptback wing with split flaps.  $R = 6,840,000$ .





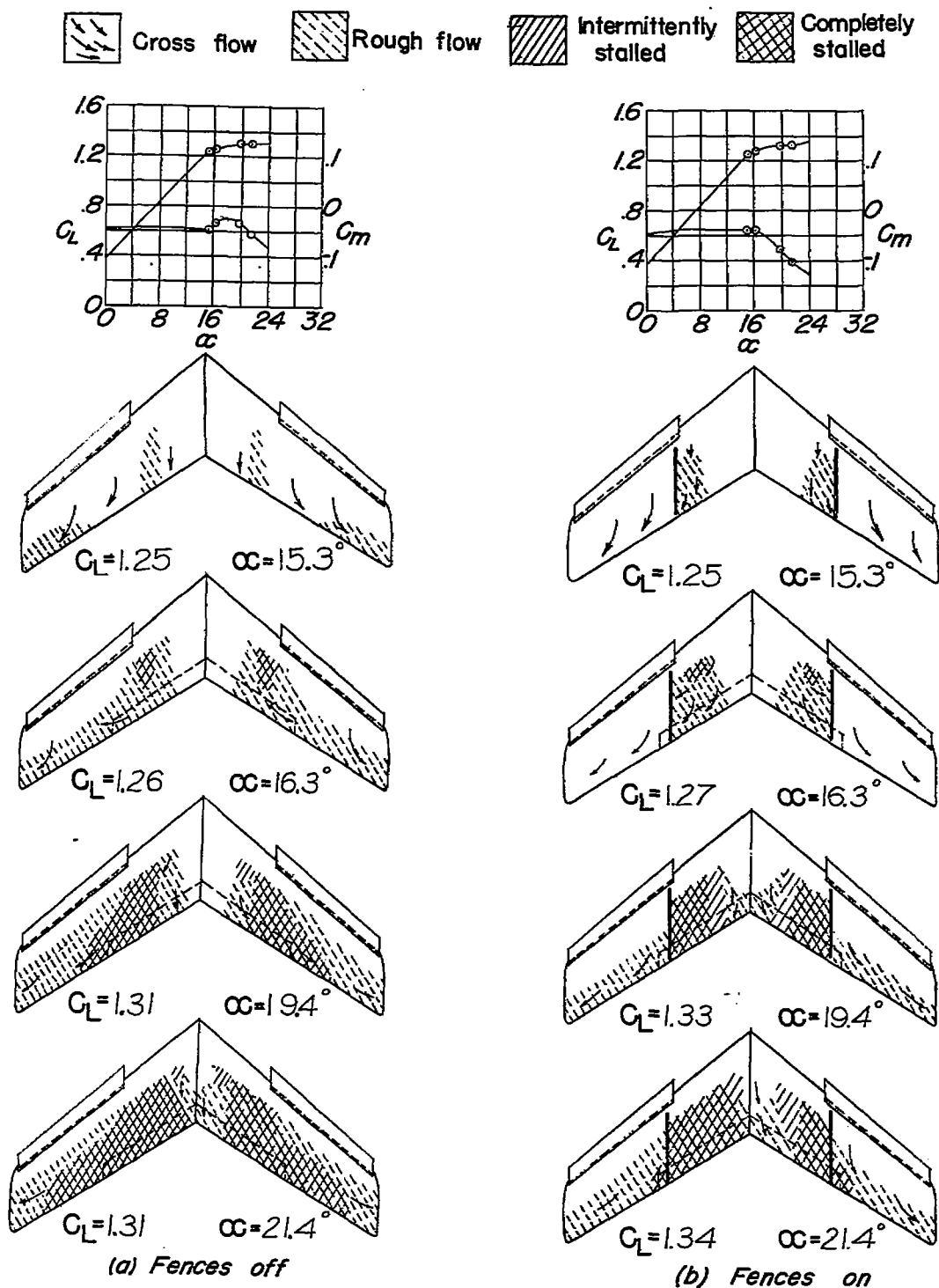


Figure 10.— Effect of upper-surface fences on stalling characteristics of  $42^\circ$  sweptback wing with  $0.575 \frac{b}{2}$  span slat and split flaps.  $R=6,840,000$ .

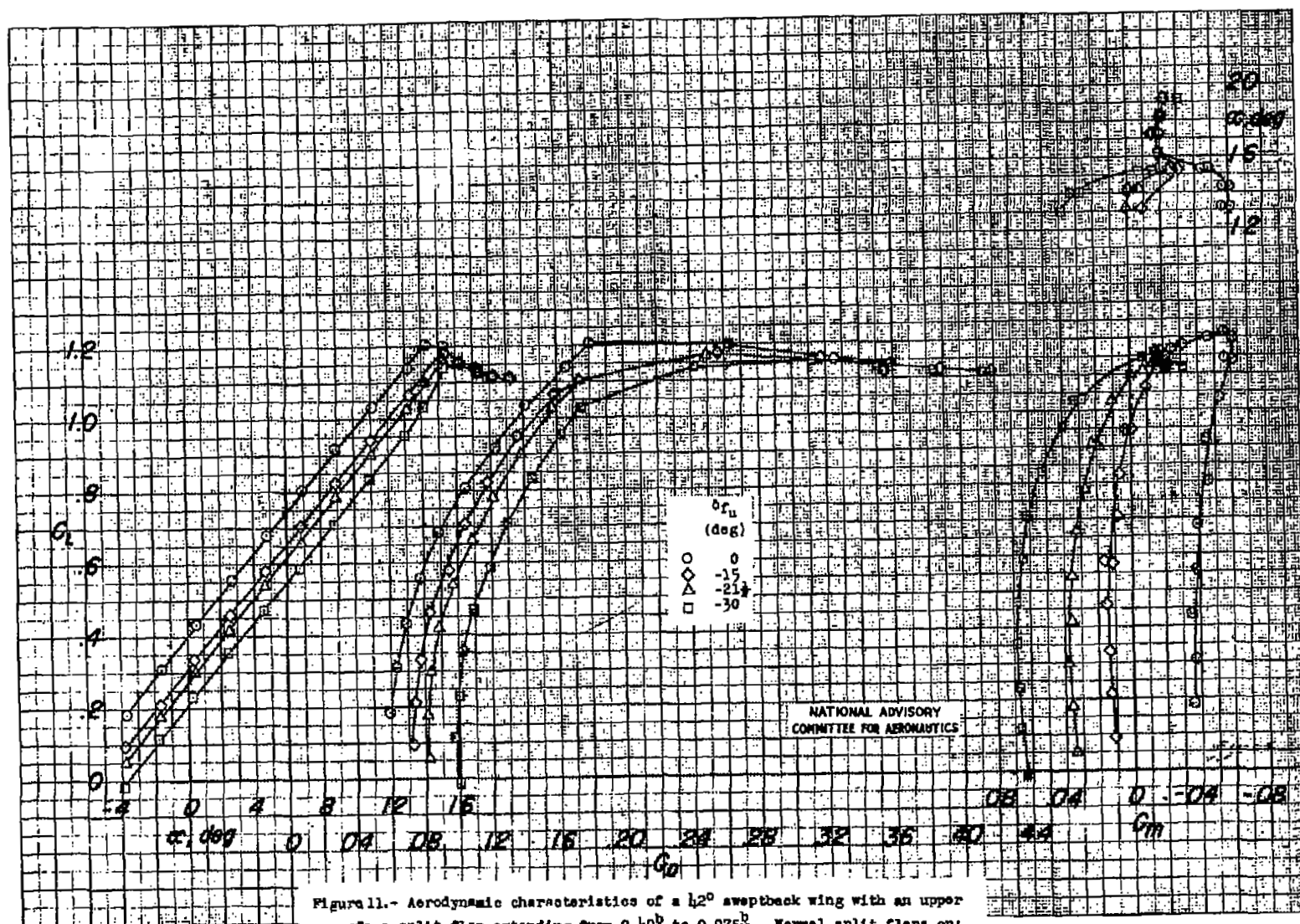


Figure 11.- Aerodynamic characteristics of a  $42^\circ$  sweptback wing with an upper surface split flap extending from  $0.40\frac{b}{2}$  to  $0.975\frac{b}{2}$ . Normal split flaps on;  $R = 6,810,000$ .

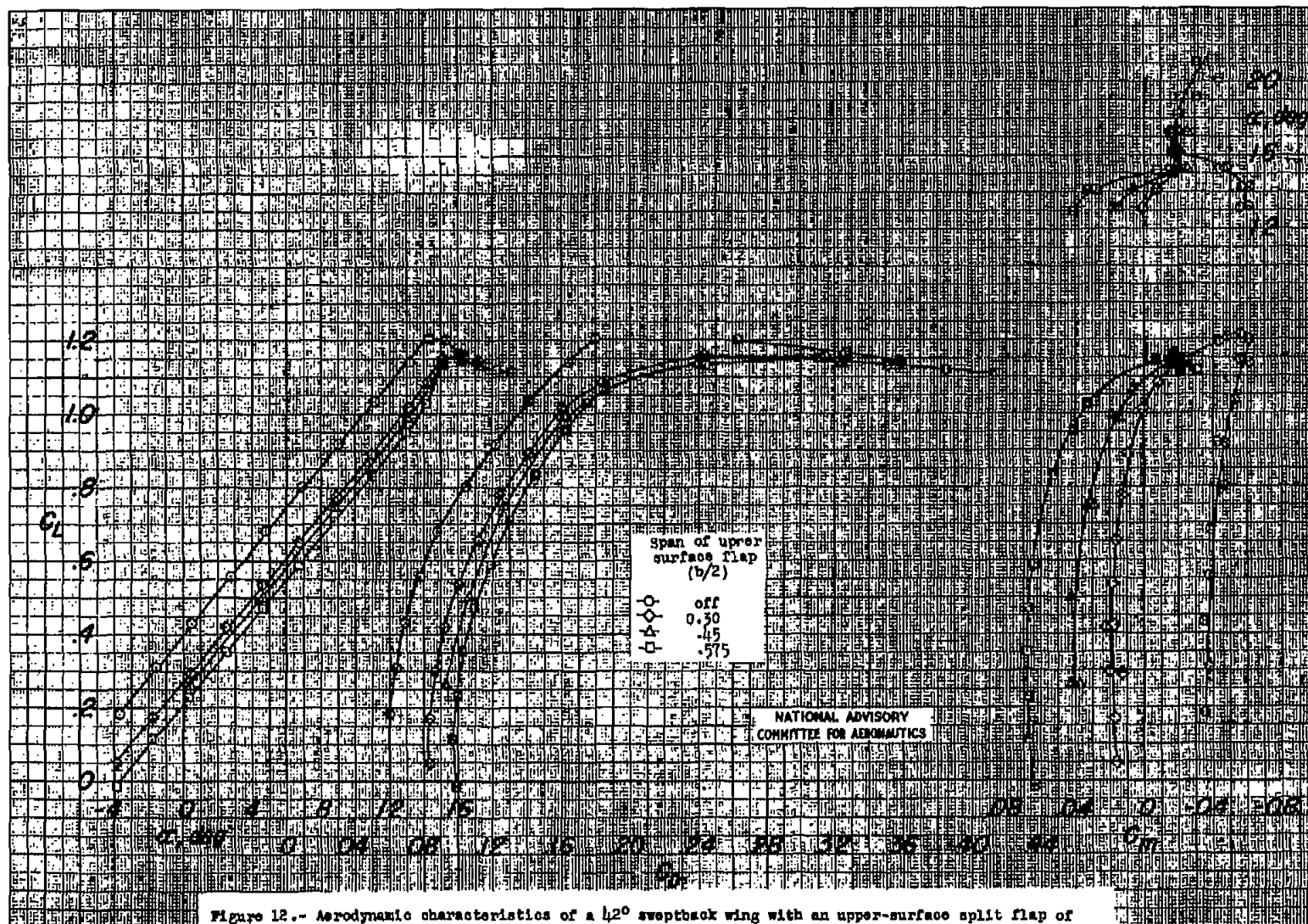


Figure 12.- Aerodynamic characteristics of a  $h_{20}$  sweptback wing with an upper-surface split flap of various spans extending outboard from  $0.40\frac{b}{2}$ .  $\delta_{fl} = -30^\circ$ ; normal split flaps on;  $R = 6,840,000$ .

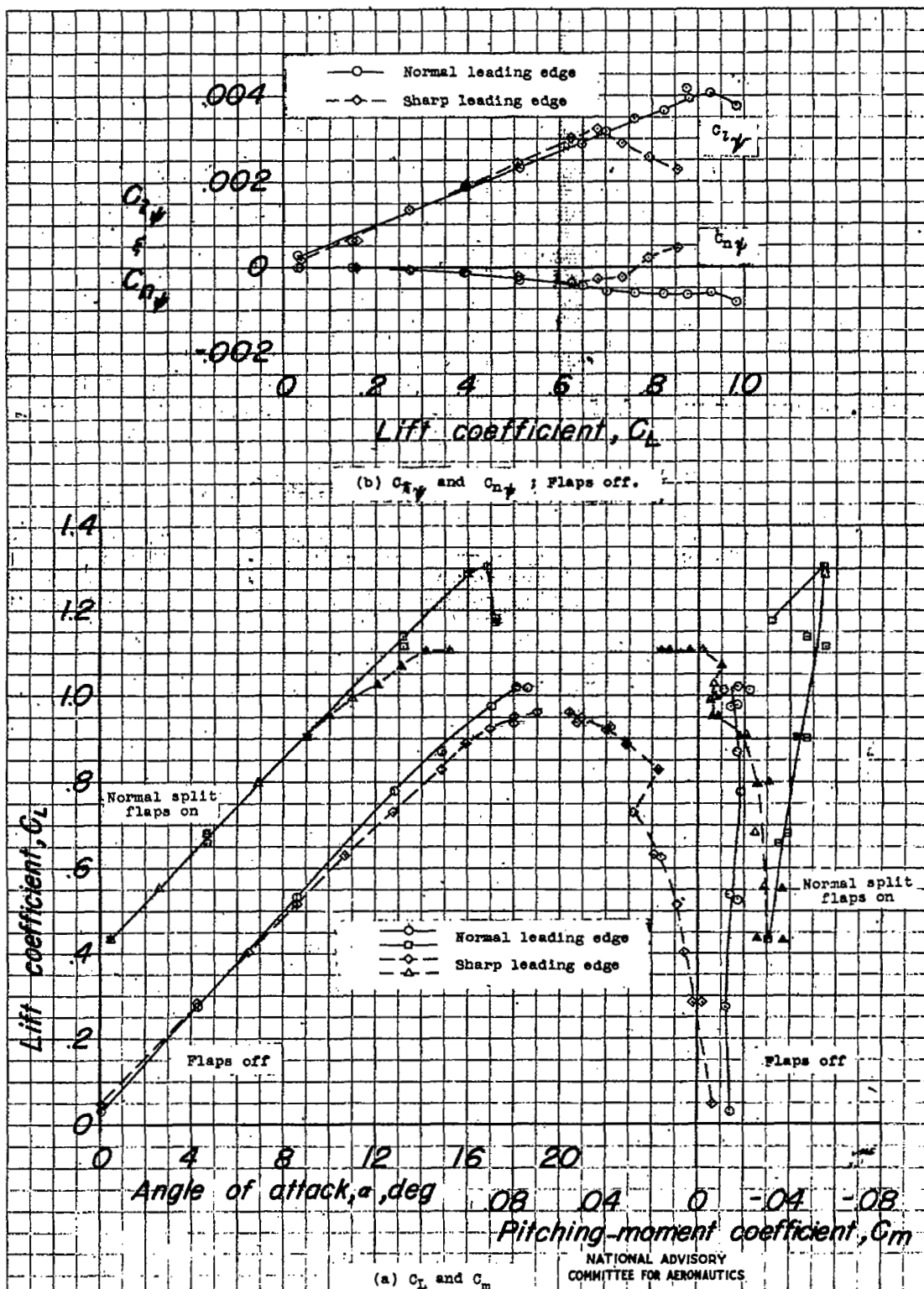


Figure 13.- Aerodynamic characteristics of a 42° sweptback wing with a simulated sharp leading edge on the inboard 50 percent of the wing.  $R = 5,300,000$ .

NATIONAL ADVISORY  
COMMITTEE FOR AERONAUTICS



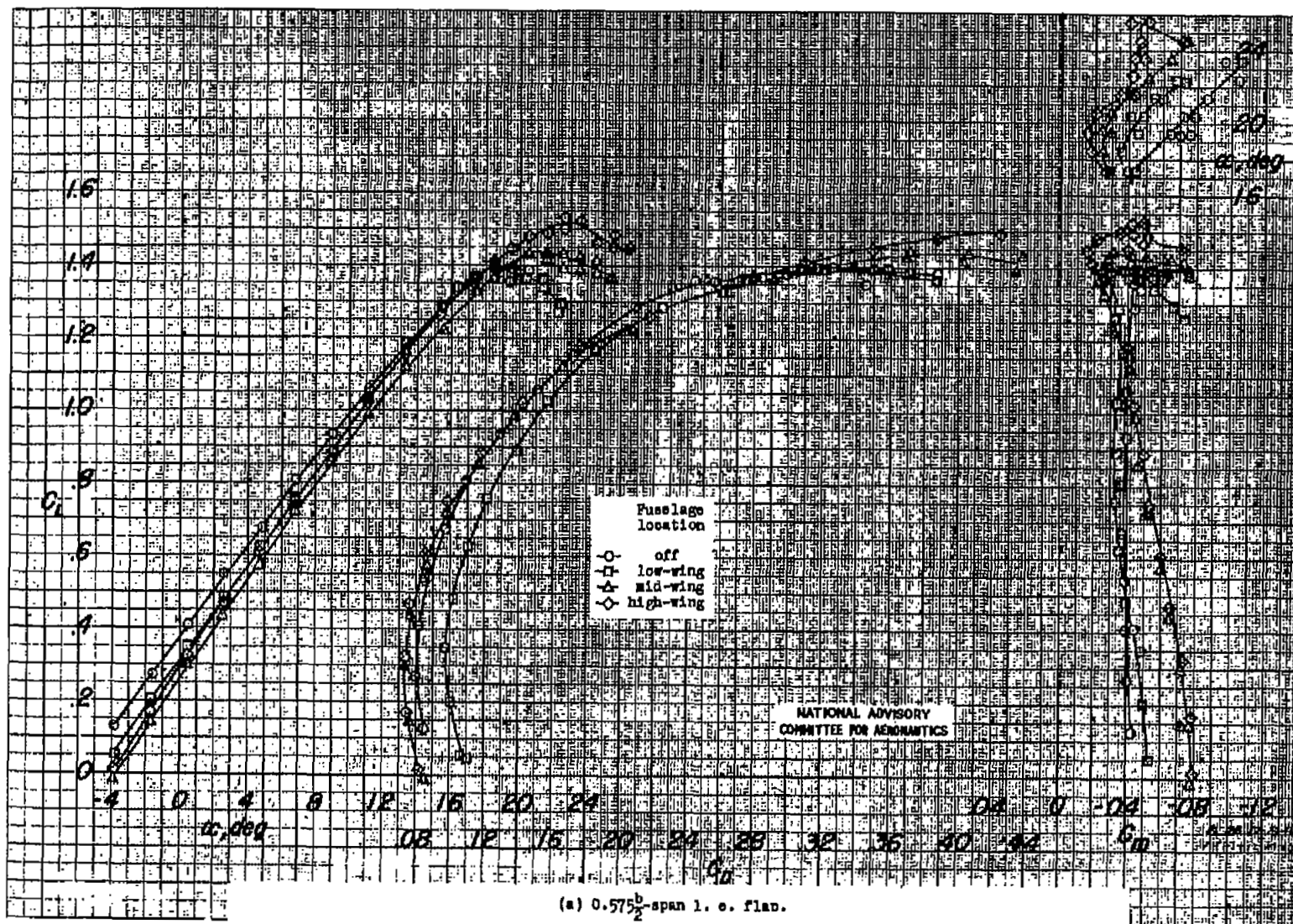


Figure 14.-- Aerodynamic characteristics of a  $42^\circ$  sweptback wing with a fuselage in various locations. Normal split flaps on;  $H = 6,840,000$ .

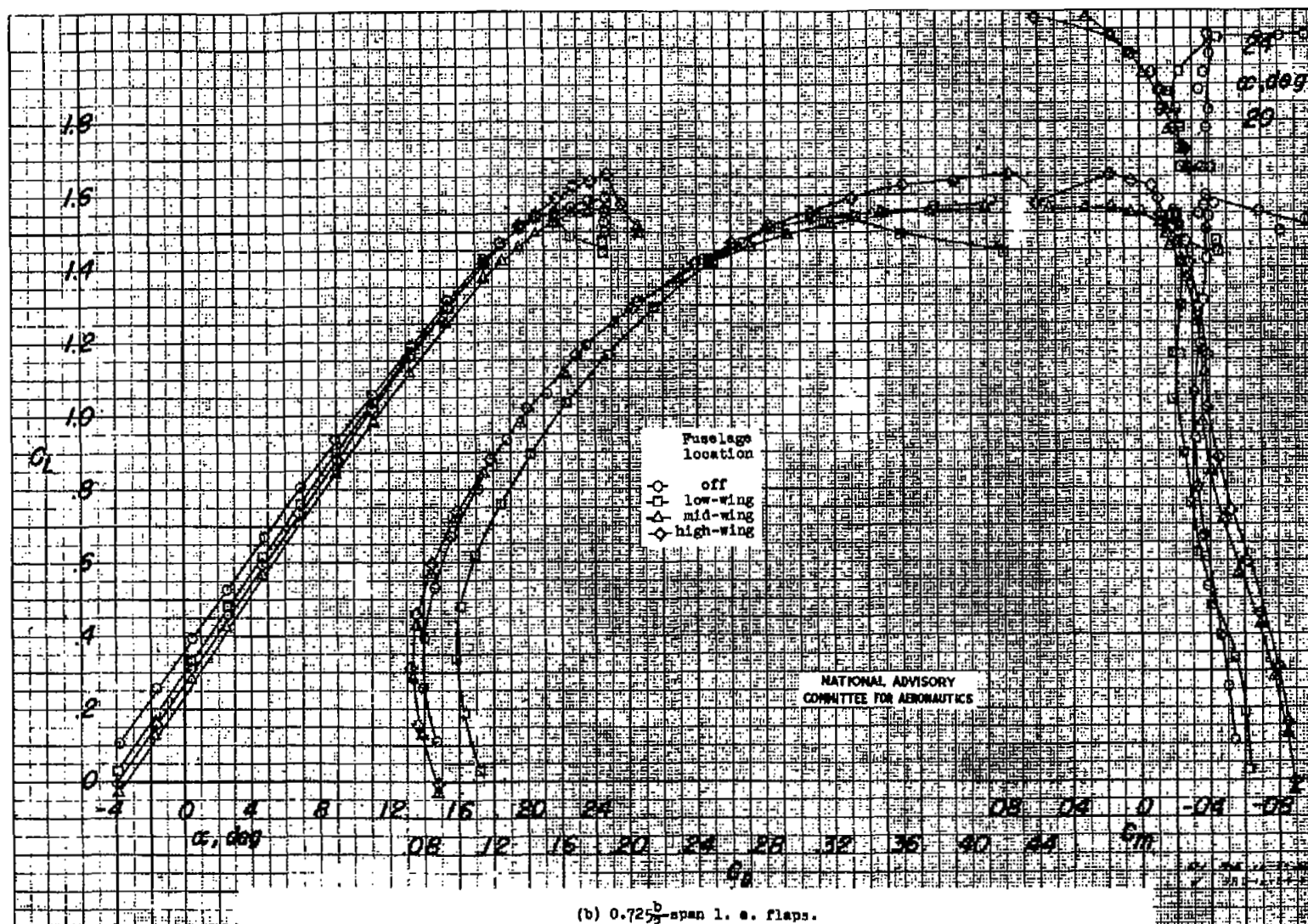


Figure 14.- Concluded.

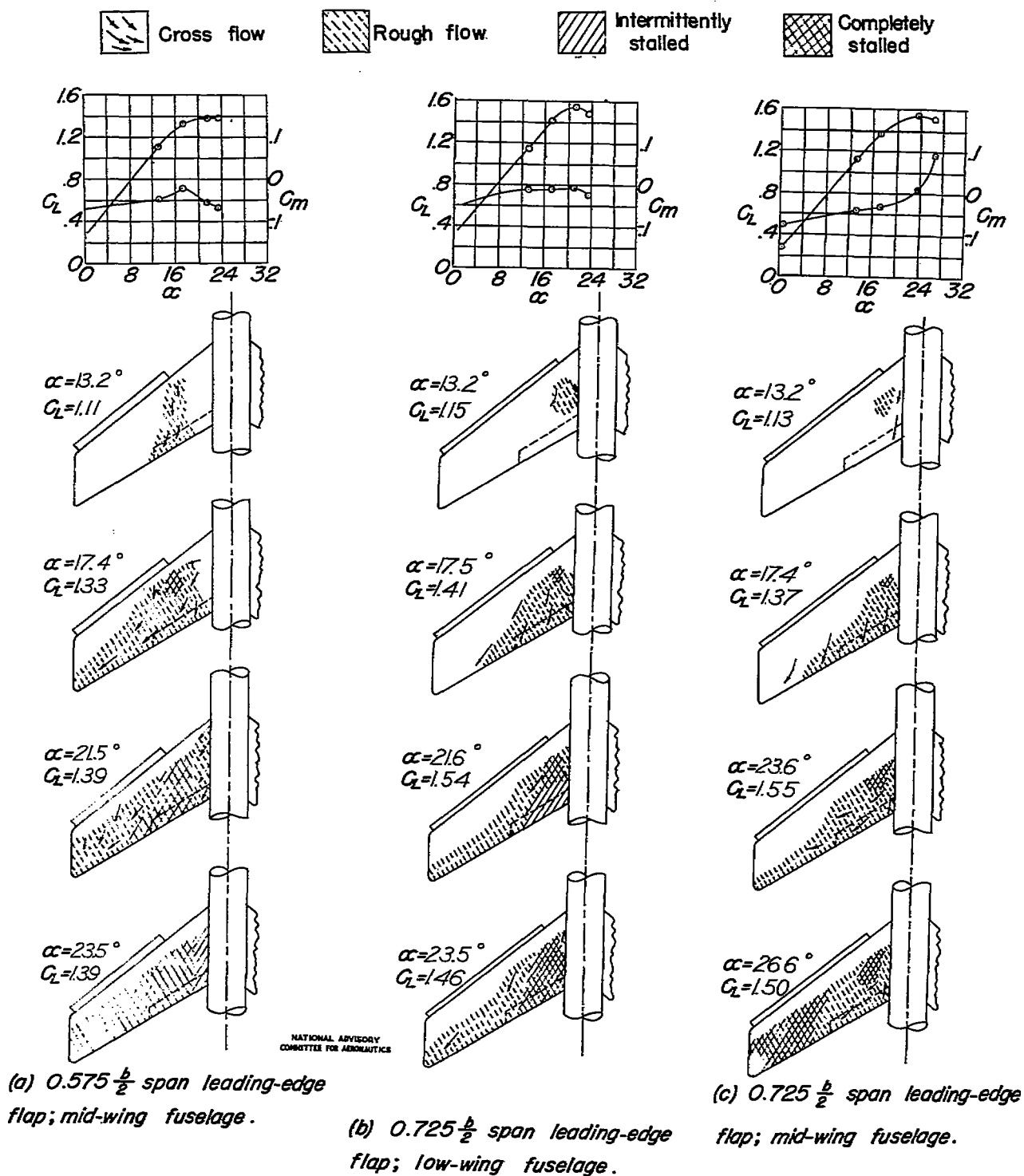


Figure 15.— Effect of leading-edge flap span and fuselage position on stalling characteristics of  $42^\circ$  sweptback wing with split flaps.  $R=6,840,000$ .



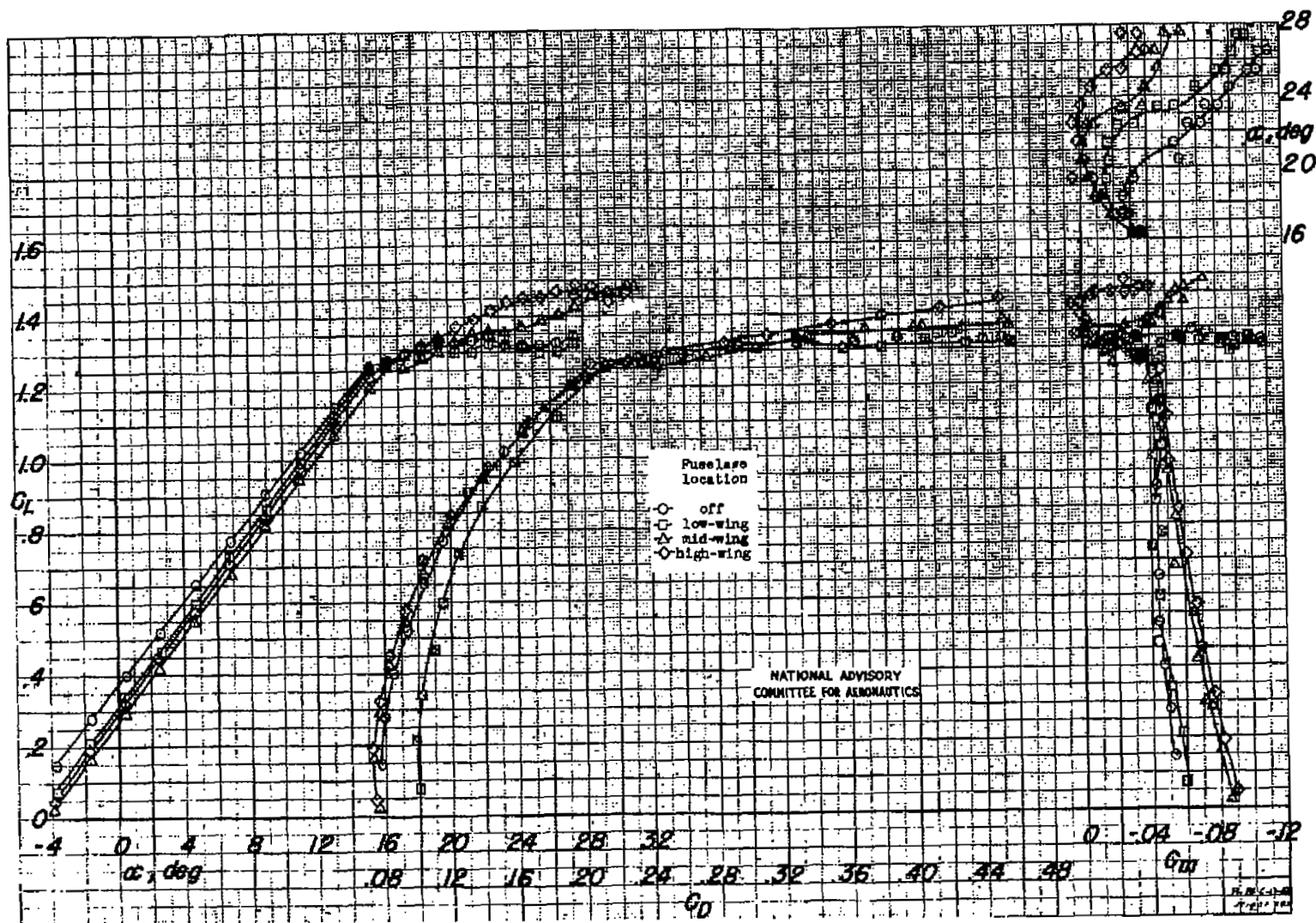


Figure 16.- Aerodynamic characteristics of a 42° sweptback wing with a  $0.575\frac{b}{2}$  span slot and a fuselage in various locations. Normal split flaps on;  $R = 6,840,000$ .

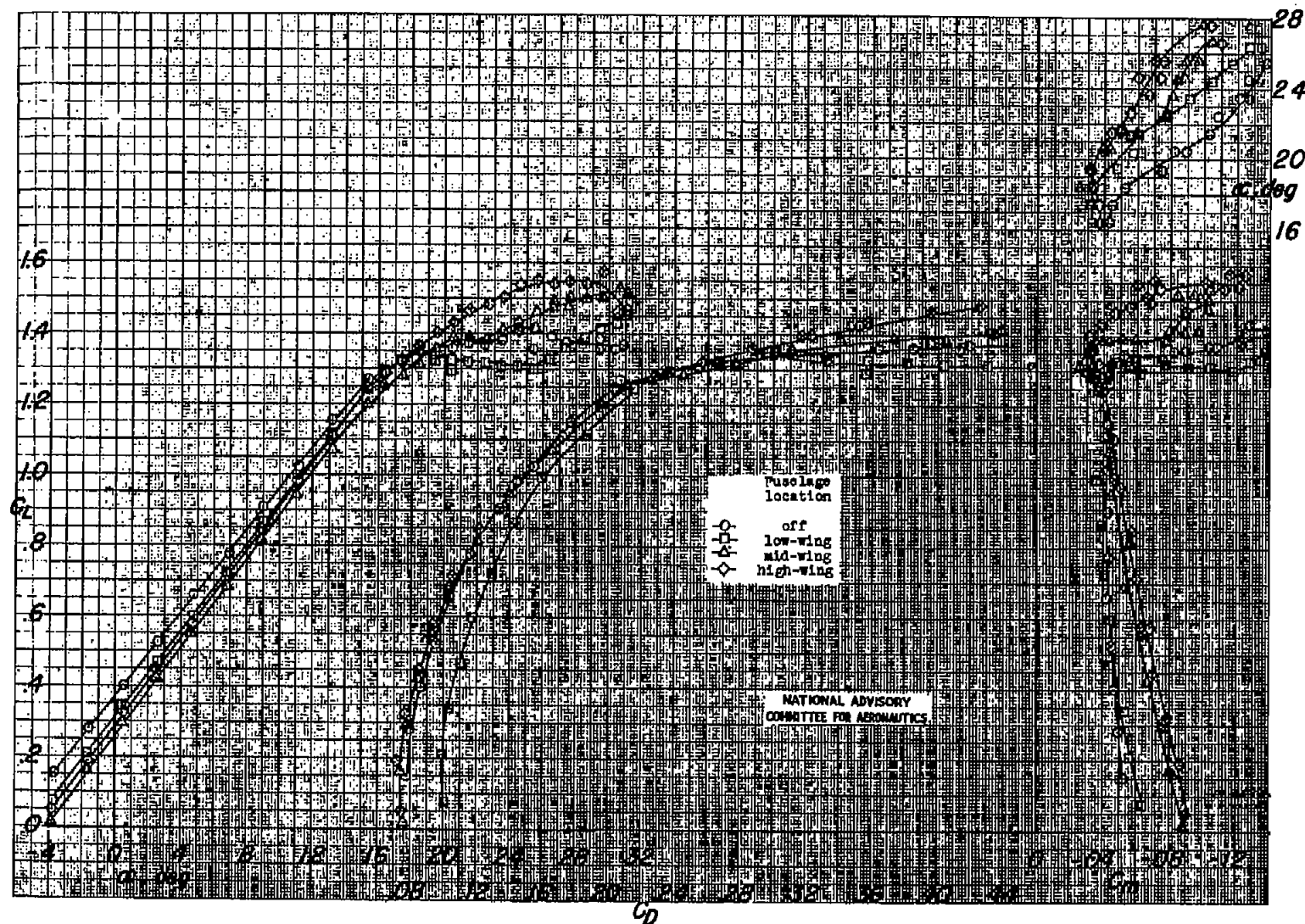


Figure 17.- Aerodynamic characteristics of a  $42^\circ$  sweptback wing with a  $0.575 b/2$ -span slat, an upper surface fence located  $0.05 b/2$  outboard of inboard end of slat, and a fuselage at various locations. Normal split flaps on;  $R = 6,840,000$



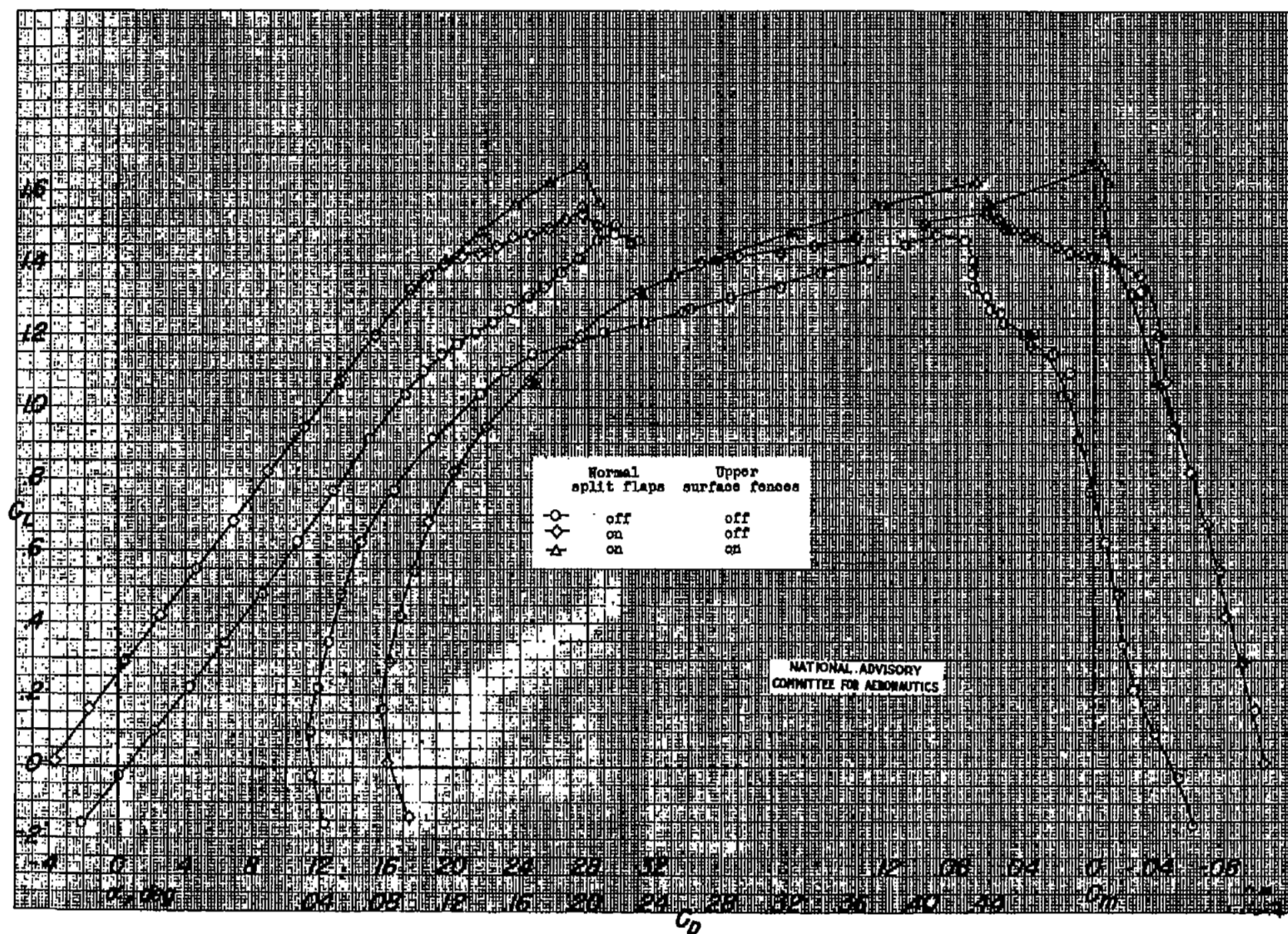
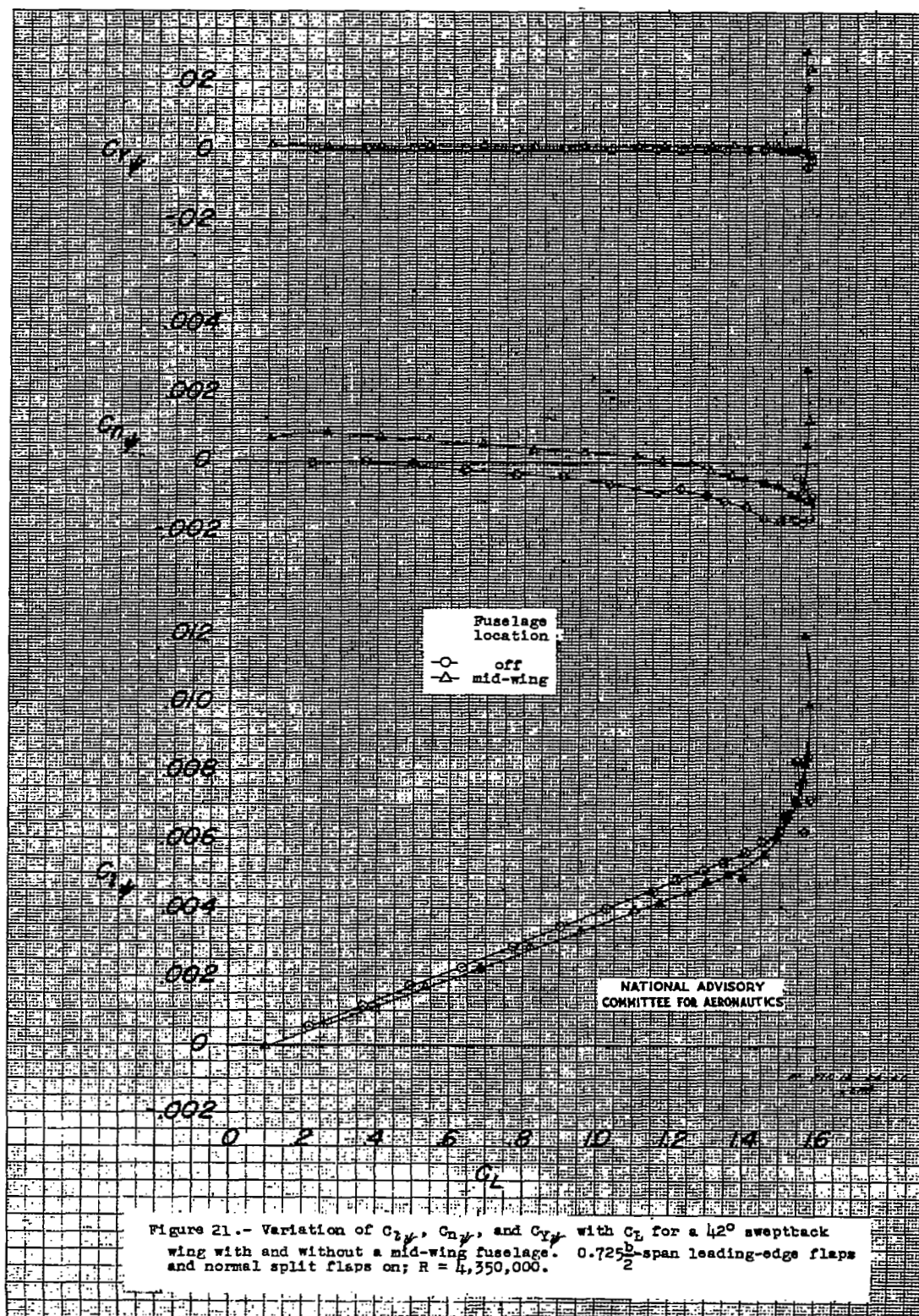


Figure 19.- Aerodynamic characteristics of a 42° sweptback wing with a 0.725-span slat and a midwing fuselage.  $R = 8,840,000$ .

•  
•  
•  
•

•  
•  
•

•  
•  
•  
•





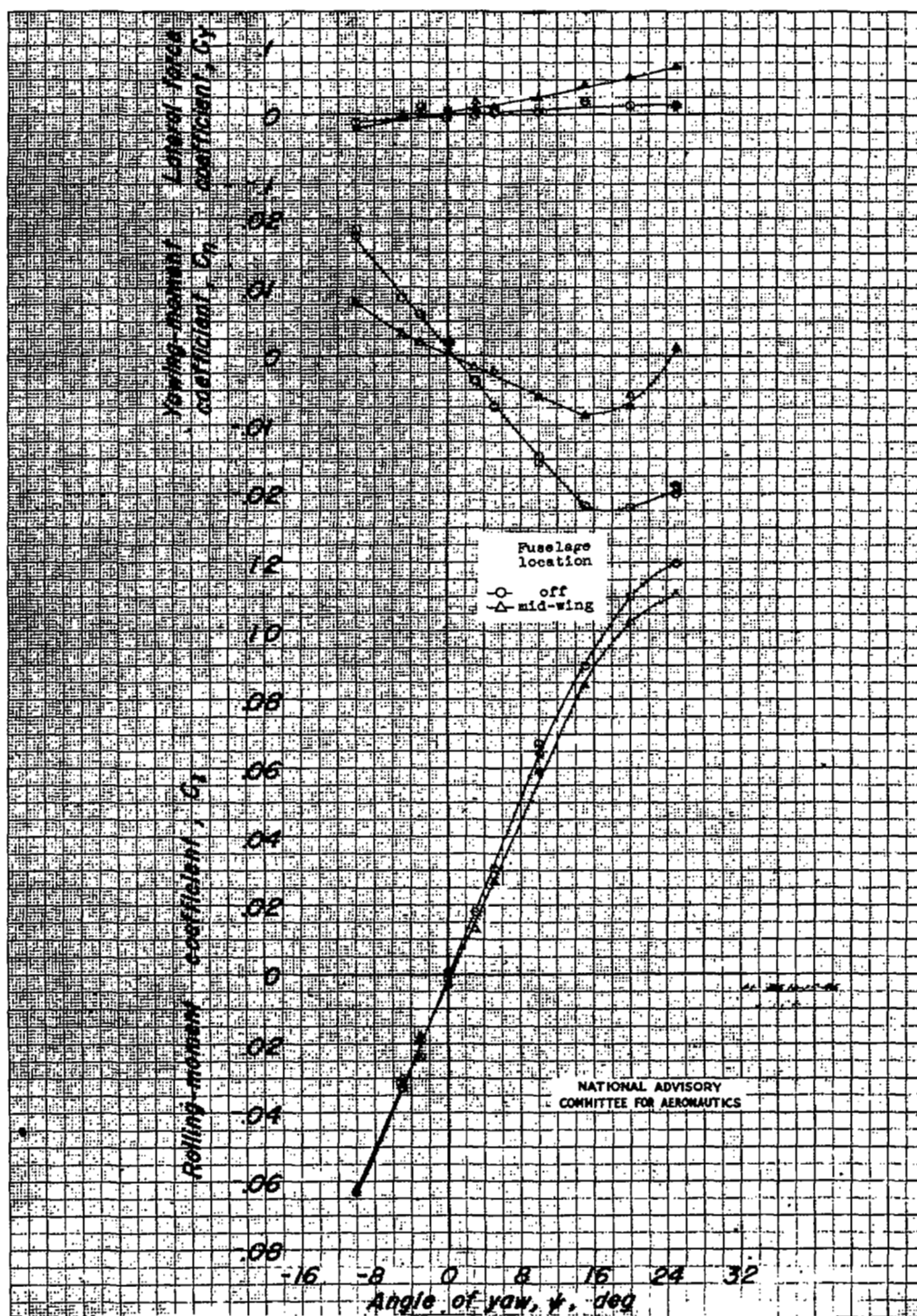
(a)  $C_Y$ ,  $C_N$ , and  $C_L$  against

Figure 22.- Aerodynamic characteristics in yaw of a 42° sweptback wing with and without a mid-wing fuselage. 0.725 $\frac{b}{c}$ -span leading-edge flaps and normal split flaps on;  $\alpha = 19.5^\circ$ ;  $R = 4,350,000$ .

